VARIATION OF THE PARTICLE CONFINEMENT DURING NEUTRAL INJECTION INTO ASDEX DIVERTOR PLASMAS

F.Wagner, K.Behringer, D.Campbell,
A.Eberhagen, G.Fußmann, O.Gehre, J.Gernhardt,
M.Kornherr, E.R.Müller, H.Rapp, G.Siller,
H.Stäbler, G.Becker, W.Engelhardt, G.v.Gierke,
G.Haas, F.Karger, M.Keilhacker, O.Klüber,
K.Lackner, G.Lisitano, G.G.Lister, H.M.Mayer,
D.Meisel, H.Murmann, H.Niedermeyer,
W.Poschenrieder, H.Röhr, J.Roth, F.Schneider,
E.Speth, K.H.Steuer, S.Succi, G.Venus
and O.Vollmer

IPP III/78 Juni 1982

MAX-PLANCK-INSTITUT FÜR PLASMAPHYSIK

8046 GARCHING BEI MÜNCHEN

MAX-PLANCK-INSTITUT FÜR PLASMAPHYSIK

GARCHING BEI MÜNCHEN

VARIATION OF THE PARTICLE CONFINEMENT DURING NEUTRAL INJECTION INTO ASDEX DIVERTOR PLASMAS

F.Wagner, K.Behringer, D.Campbell,
A.Eberhagen, G.Fußmann, O.Gehre, J.Gernhardt,
M.Kornherr, E.R.Müller, H.Rapp, G.Siller,
H.Stäbler, G.Becker, W.Engelhardt, G.v.Gierke,
G.Haas, F.Karger, M.Keilhacker, O.Klüber,
K.Lackner, G.Lisitano, G.G.Lister, H.M.Mayer,
D.Meisel, H.Murmann, H.Niedermeyer,
W.Poschenrieder, H.Röhr, J.Roth, F.Schneider,
E.Speth, K.H.Steuer, S.Succi, G.Venus
and O.Vollmer

IPP III/78 Juni 1982

Die nachstehende Arbeit wurde im Rahmen des Vertrages zwischen dem Max-Planck-Institut für Plasmaphysik und der Europäischen Atomgemeinschaft über die Zusammenarbeit auf dem Gebiete der Plasmaphysik durchgeführt.

IPP III/78

VARIATION OF THE PARTICLE CONFINEMENT DURING NEUTRAL INJECTION INTO ASDEX DIVERTOR PLASMAS

F.Wagner, K.Behringer, D.Campbell, A.Eberhagen, G.Fußmann, O.Gehre, J.Gernhardt, M.Kornherr, E.R.Müller, H.Rapp, G.Siller, H.Stäbler, G.Becker, W.Engelhardt, G.v.Gierke, G.Haas, F.Karger, M.Keilhacker, O.Klüber, K.Lackner, G.Lisitano, G.G.Lister, H.M.Mayer, D.Meisel, H.Murmann, H.Niedermeyer, W.Poschenrieder, H.Röhr, J.Roth, F.Schneider, E.Speth, K.H.Steuer, S.Succi, G.Venus, O.Vollmer

May 1982

Abstract

With neutral injection into ASDEX divertor plasmas the line average density generally decreases. Evidence is presented that the reduction in plasma content is partly caused by a reduction in particle confinement. The reduction in confinement affects the outer plasma zones first, and frequently, in conjunction with a sawtooth instability, impairs the plasma center too. The overall reduction in particle confinement is not caused by beam effects alone but appears to be correlated with profile changes of the heated plasma. The deterioration of the particle confinement does not seem to be an inevitable occurrence. There exists an operational regime where the density increases during the neutral injection pulse after first decreasing in the usual manner. Under these circumstances the density increase leads to high β_p values of about 1.55 to 1.75 and a threefold enhanced neutron flux. The high β_p-phase is periodically interrupted by gross instabilities in the outer plasma zones which cause sudden β_p-reductions.

CONTENTS

1. INTRODUCTION

During neutral injection (NI) in ASDEX divertor plasmas generally the plasma density decreases even with the gas flux Φ_G from the external gas valve kept constant and the additional particles deposited within the plasma by the beam. An example of the time variation of the line average density $\bar{n}_e$ measured along a chord through the plasma center is plotted in Fig.1. $\bar{n}_e$ decreases from $3.7 \times 10^{13} cm^{-3}$ during the ohmic phase to $2.4 \times 10^{13} cm^{-3}$ with neutral injection (the injection phase is indicated by a hatched area in this and the following figures). Φ_G is not regulated by a feedback system during the NI-pulse but is held constant during neutral injection at the level which maintains a density plateau in the ohmic phase. Φ_G is about 3.5×10^{21} atoms/sec in the case shown in Fig.1 with 1.2 MW injection power. The neutral source introduces $\Phi_B \sim 3.1 \times 10^{20}$ fast atoms/sec and a negligible flux of cold atoms. When the beam is turned off (arrow 1 in Fig.1) the density decreases even further before the density feedback system is activated again (at arrow 2) to restore the density to the original value.

The loss of plasma particles during neutral injection is particularly severe at medium plasma densities. At low density ($\bar{n}_e \sim 1 - 2 \times 10^{13} cm^{-3}$) the plasma density stays constant; at high density ($\bar{n}_e \sim 7 \times 10^{13} cm^{-3}$) the relative decrease in density with neutral injection is small: $\Delta\bar{n}_e/\bar{n}_e \leq 0.1$.

From other tokamaks like ISX-B /1/ or DITE /2/ it is known that the plasma density during neutral injection could only be increased by strongly enhanced gas puffing from the outside. This phenomenon has been called "density clamping". In Ref./3/ "density clamping" is partly explained by a reduction of the recycling coefficient of the working gas during neutral injection.

The possibility that the density decrease is caused by a reduction of the recycling coefficient r or that it is in case of ASDEX a divertor related phenomenon will be briefly discussed. The main purpose of this report, however, is to present evidence that the particle confinement decreases during neutral injection, to indicate the correlation with MHD-effects,and finally,to demonstrate that it is possible for the confinement to improve again during the injection phase.

2. THE NEUTRAL INJECTION SYSTEM OF ASDEX

The neutral injection system of ASDEX comprises two beam lines each delivering about 1.2 MW injection power into the plasma for 2oo msec at 4o kV source voltage. Both beam lines are oriented near-tangential and inject parallel to the direction of the plasma current (co-injection).

In all cases described here neutral injection experiments have been conducted solely in divertor discharges with single- or double null configuration. In all cases presented the target plasma has been deuterium heated by hydrogen beams. Titanium is occasionally evaporated moderately in both divertor chambers. The details of the injection system are outlined in Ref. /4/.

3. BRIEF SUMMARY ON REDUCTION IN RECYCLING COEFFICIENT AND REFUELING EFFICIENCY WITH NEUTRAL INJECTION

The actual plasma content at a given external gas flow Φ_G is determined by the effective particle confinement time τ_p^* which includes wall recycling. Owing to desorption and backscattering from the wall τ_p^* is much larger than the inherent magnetic con-

finement τ_p. This pertains for limiter as well as divertor discharges. The difference in recycling between both configurations is that the immediate hydrogen exchange occurs between the plasma and the wall, particularly the limiter in limiter discharges /5/. In a divertor discharge the main recycling occurs between plasma and divertor chambers which are filled with hydrogen in the course of the discharges /6/. Hydrogen streams back from the divertor chambers and refuels the main plasma.

The particle content N of a divertor plasma is determined by the global particle confinement time τ_p of the plasma within the separatrix, the recycling coefficient r and the actual external gas flux $\gamma\Phi_G$ which fuels the plasma:

$$N \simeq \frac{\tau_p}{1-r}[\gamma\Phi_G + \Phi_B]$$

γ is the fueling efficiency which is experimentally found to be smaller than 1 for divertor plasmas /7/. Φ_B is the atom flux due to the NI-beams.

The reduction of one of the coefficients τ_p, r or γ causes a decrease of the plasma content at constant external gas flow.

- A reduction of r can be expected during neutral injection. The temperature of the hot ion component in the boundary plasma, measured within the divertor chamber by a charge exchange analyzer, increases from typically 80 eV to 150 eV with neutral injection. From the increase in average energy of the ions and atoms hitting the wall, a reduction in recycling coefficient can be expected as the backscattered and the desorbed flux from the wall decrease, the latter

because of a deeper hydrogen deposition within the wall. A decrease in r is manifested experimentally too. There are neutral injection cases in which the divertor plasma line density and the hydrogen pressure within the divertor chamber decrease together with the plasma content though the external gas flow is constant. Obviously the hydrogen content of the wall increases on account of the hydrogen content of plasma, boundary layer and divertor. This can be described by a lower recycling coefficient.

- A further cause for the density decrease during neutral injection could be a reduction of the fueling efficiency particularly as it is observed that the electron temperature of the boundary layer increases with neutral injection. The increase in electron temperature may enhance the ionization processes within the boundary layer on account of dissociation processes /8/. Thereby the flux of Frank-Condon atoms into the main plasma may be reduced.

An increase of the external gas flux Φ_G by a factor of 3 during neutral injection can reduce the amount of density decrease but it cannot prevent it. However, the enhanced gas flux sharply increases the boundary layer density as measured within the divertor chamber. Though the boundary layer density does not explicitly depend on the refueling efficiency, this behavior, particularly in comparison with the relatively moderate effect on the main plasma density, may imply a decrease of γ during neutral injection. Thereby the external gas flux and probably the recycling flux too, becomes less effective for refueling the main plasma.

4. VARIATION OF THE PARTICLE CONFINEMENT TIME DURING NEUTRAL INJECTION

4.1 Decrease of τ_p at the beginning of neutral injection

- Variation of the boundary layer density

Figure 2a shows the decrease of the line density of the main plasma and Fig.2b the variation of the boundary layer density measured in the divertor chamber during neutral injection. The main plasma line density is measured along three horizontal chords, one through the plasma center, one through $z = a/2$ and one through $z = 3/4$ a (minor radius $a = 4o$ cm). Figure 2b shows the density trace of the outer channel of the lower divertor chamber.

The main plasma density decreases shortly after the beginning of the injection. The density along the outer chord ($z = 3/4a$) decreases 8.5 msec after the voltage to the injector source has been applied. The density along the middle chord ($z = 1/2a$) decreases somewhat later after 13 msec. The density through the center seems to decrease even later; a sharp discontinuity as in the other 2 cases, however, cannot be defined.

A different behaviour is shown by the boundary layer density. It starts to increase 6 msec after the beginning of neutral injection. At that moment the hard X-ray radiation increases too, indicating that runaway electrons are lost from the plasma to the wall. The decrease in plasma density and the loss of runaway electrons is indicative of a loss of particle confinement. The deterioration of the confinement seems to start shortly after initiation of the beams first at the plasma edge from where it proceeds toward the plasma interior.

The variation of the boundary layer density supports the concept of a τ_p-reduction. The sudden increase in boundary layer density may originate from an enhanced particle efflux from the main plasma into the boundary layer till a new equilibrium is established.

The particle balance equation for the divertor plasma within the separatrix in a divertor tokamak can be written:

$$\frac{dN}{dt} + \frac{N}{\tau p} = \gamma(\phi_G + \phi_D) \quad [+ \phi_B] \tag{1}$$

ϕ_D is the recycling flux from the divertor chambers. Within the short time scale of Fig.3 the neutral pressure of the divertor chamber does not change so that ϕ_D is treated as constant. With NI the atom flux ϕ_B from the beam has to be added.

The particle balance equation of the boundary layer plasma is written:

$$\frac{dn}{dt} + \frac{n}{\tau^*_{\shortparallel}} = (1-\gamma)(\phi_G + \phi_D) + \frac{N}{\tau_p} \tag{2}$$

n is the particle content of the boundary layer plasma, $\tau^*_{\shortparallel}$ is the effective confinement time of the boundary plasma given by the drift time from the main plasma to the neutralizer plate and incorporating the local recycling of the boundary layer plasma within the divertor.

The stationary solutions N_o and n_o of the equations (1) and (2) are:

$$\begin{aligned} N_o &= \tau_p \gamma \ (\phi_G + \phi_D) \ [+ \tau_p \ \phi_B] \\ n_o &= \tau^*_{\shortparallel} \ (\phi_G + \phi_D \ [\ + \phi_B \ ]) \end{aligned} \tag{3}$$

If we assume that at t = 0 the particle confinement time τ_p is reduced from τ_{p1} to τ_{p2}, then the plasma content decreases with time:

$$\frac{N(t)}{N_o} = \frac{\tau_{p2}}{\tau_{p1}} + \left(1 - \frac{\tau_{p2}}{\tau_{p1}}\right) e^{-t/\tau_{p2}} , \tag{4}$$

and decays to:

$$N_\infty = N_o \frac{\tau_{p2}}{\tau_{p1}} . \tag{5}$$

The decay time τ_{eff} of the plasma content at t = 0 is:

$$\tau_{eff} \equiv \frac{-N_o}{\frac{dN}{dt}(t=0)} = \frac{\tau_{p1}\tau_{p2}}{\tau_{p1}-\tau_{p2}} \tag{6}$$

The time variation of the boundary layer content is:

$$\frac{n(t)}{n_o} = 1 + \gamma \frac{\tau_{p1}-\tau_{p2}}{\tau_{p2}-\tau_{\shortparallel}^*} \left(e^{-t/\tau_{p2}} - e^{-t/\tau_{\shortparallel}^*}\right) \tag{7}$$

$\frac{n}{n_o}$ has a maximum at $t = t_M = \frac{\tau_{p1}\,\tau_{\shortparallel}^*}{\tau_{p2}-\tau_{\shortparallel}^*} \ln \frac{\tau_{p1}}{\tau_{\shortparallel}^*}$ (8)

At a line average density $\bar{n}_e = 3.7 \times 10^{13} cm^{-3}$ a particle confinement time $\tau_{p1} = 35$ msec is assumed /6/. From eqs.(5) and (6) and the density as plotted in Fig.2 τ_{p2} can be estimated. An average value $\tau_{p2} = 25$ msec is used in the following. As the density profile peaks during the phase of decreasing confinement the actual plasma outflux N/τ_{p2} may be higher than computed from the decrease of the line average density. At present, accurate density profiles during neutral injection are not available.

$\tau_{\parallel}^{*}$ can be estimated from those cases with strong sawtooth oscillations during neutral injection. During a sawtooth relaxation part of the plasma content is expelled into the boundary layer and transiently increases the density there. The decay of this density pulse occurs within approximately 1o msec which is identified with $\tau_{\parallel}^{*}$.

The dashed curves in Fig.2a and b show the relative variation of the main plasma density and the boundary layer density calculated from eqs. (4) and (7) assuming $\gamma = 0.4$ /7/.

Though there are discrepancies in the exact description of the time variation of the two densities the occurrence of a maximum in the boundary density after the estimated time lapse and with the expected relative height supports the concept of reduced particle confinement. An exact description cannot be expected from this simplistic treatment (sudden decrease in τ_p and assuming $dN/dt \propto d\bar{n}_e/dt$) which ignores effects caused by changes in recycling coefficient and refueling efficiency.

However, it can be ruled out that the peak in boundary layer density is caused by the outward displacement of the plasma column when the beam is switched on (see Fig.13). A simulation of the same shift caused not by the beams but by a sudden decrease of the vertical field showed no effect on the boundary layer density.

The filling of the NI source and neutralizer cell with gas - another potential source for the boundary layer density variation - occurs 2oo msec prior to injection and does not affect the boundary layer density.

A peak in the boundary layer density as shown in Fig.2b is observed during neutral injection into double null divertor discharges with constant external gas flux during injection, and without strong sawtooth activity. Otherwise the maximum in boundary layer density is masked by a sharp increase or by inverse sawtooth fluctuations in some cases with large amplitudes.

- Measurement of the volume ionization rate.
  During the density plateau phase, the volume ionization rate

$$\int n_o n_e \langle \sigma v \rangle_i dV \qquad (9)$$

(n_o = neutral density, $\langle \sigma v \rangle_i$ = ionization rate coefficient) balances the ion efflux N/τ_p across the separatrix. In order to maintain a constant plasma content with a reduced confinement time an enhanced ionization rate is required. The ionization rate is proportional to the H_α/D_α-radiation.(As the neutral injection experiments are generally carried out with H^o-beams fired into D^+-plasmas, sensors are used which measure the sum of H_α- and D_α-radiation.) In order to estimate the volume ionization rate several H_α-monitors have to be placed around to torus. Measurements show that the H_α-intensity from this part of the plasma where neutral injection occurs increases sharply owing to the ionization of beam and cold atoms from the source. The variation of the H_α/D_α-intensity far away from the neutral beam has been measured by H_α-monitors 180^o, 200^o and 245^o in toroidal direction away from the injection port. Figure 3 shows the signals of the H_α-monitors at about 200^o (solid line) and 245^o (dashed line) toroidal distance together with the plasma density (both H_α-monitors are also far away from the gas input valve).

The H_α/D_α-intensity increases at all representative toroidal positions so that it can be concluded that the volume ionization rate increases. Nevertheless, the density decreases, confirming the hypothesis of a particle confinement time reduction during neutral injection.

- Measurement of the hard X-ray radiation

In Fig.4 the time variation of the line averaged plasma density $\bar{n}_e$, the plasma current I_p and the hard X-ray counting rate $\dot{N}_x$ is plotted during 3 phases of the discharge - the built-up phase, the current and density plateau at the time of neutral injection (on an expanded time scale), and finally the termination of the discharge.

The decrease in density during neutral injection is accompanied by a sharp rise in the hard X-ray counting rate. It results from runaway electrons striking obstacles at the vessel wall (such as auxiliary limiters 1o cm away from the separatrix). As there is no further hard X-ray burst at the end of the discharge, as normally occurs, it is concluded that all runaway electrons are lost during neutral injection. The fluences of the hard X-ray radiation of a discharge with NI and the same type of discharge without NI are about the same. The hard X-ray radiation sets in shortly after the initiation of neutral injection at a time correlated with the decrease in plasma content. Like in the case of the boundary layer density it is experimentally checked that the radial expansion of the plasma column does not cause the sudden increase in hard X-ray flux.

The obvious decrease of the particle confinement time with neutral injection also affects the confinement of the runaway electrons. This sheds some light on the nature of the deterioration in confinement which could be caused by a partial ergodisation of the magnetic field lines and the formation of islands (other mechanisms which enhance cross-field, transport, however, cannot be excluded).

Additional experimemtal results which indicate a reduction in particle confinement during NI are summarized here without further discussion. The parallel flux of ions to carbon collector probes exposed in the space between plasma and vessel wall increases typically by an order of magnitude during neutral injection. Similarly, the pressure at the vessel wall measured by a shielded ionization gauge increases . It is further observed that an additional plasma density increase by pellet injection relaxes faster to its equilibrium value with neutral injection than during the ohmic phase / 9 /. At present, however, it is not clear to what extent this reduction in relaxation time reflects the reduced particle confinement by the beam. There are indications that the pellet is ablated more rapidly with neutral injection and is therefore deposited in outer plasma zones where the particle confinement is lower.

For the future application of auxiliary heating by neutral injection it is important to know whether the decrease in particle confinement is unavoidable, whether it occurs due to beam-plasma interaction, or whether it is a corollary of the heated plasma. The following summarizes contributions to these questions.

4.2 Does the beam deteriorate the particle confinement

Generally, the density decreases shortly after the beginning of neutral injection. There are cases, however, where the central density decrease is delayed. Figure 5 shows the line average density measured through the plasma center ($z = 0$) and measured through $z = a/2$, the H_α/D_α-intensity of the main plasma and the hard X-ray radiation $\dot{N}_x$. The density through $z = a/2$ starts

to decrease shortly after the beginning of neutral injection, and the hard X-ray radiation increases somewhat. The central line density, however, stays constant for a further 35 msec despite the decrease in line density of the peripheral zones. During this phase, the density profile seems to peak. Thus outer plasma zones are first affected by the deterioration in confinement (see also Fig.2a). After 35 msec a sawtooth relaxation occurs in the plasma center, which causes the central density to decrease too. The inverted sawtooth is seen from the line density along the chord $z = a/2$; sawtooth and inverted sawtooth are also observed in the electron temperature as measured by electron cyclotron emission. The sawtooth relaxation causes a further particle loss. Part of the expelled ions recycle at the wall and give rise to a peak in the H_α/D_α-intensity. Part of the lost plasma is caught by the boundary layer and transported into the divertor where it gives rise to a similar peak in the boundary layer density. The hard X-ray radiation indicates, that runaway electrons are lost from the plasma due to the single sawtooth relaxation.

The delay of the dominant particle loss from the plasma center by 35 msec, caused by, or at least correlated with, a sawtooth relaxation, is sufficient to allow the injection beams to come into equilibrium, cause plasma rotation (up to now no direct observation) or to increase the plasma temperatures. The partial delay in the decrease of particle content seems to indicate that the beam itself does not necessarily impair the particle confinement in the plasma center.

The occurrence of a density decrease is independent of the injected power. Figure 6 shows the variation of the line density measured horizontally along $z = a/2$ for three different injec-

tion powers. At low power (0.6 MW) the density decreases more slowly than in the high power case (2.6 MW) but it falls to a lower value than at high power possibly because more beam particles are deposited within the plasma at higher power.

In conclusion, the plasma seems to be in a marginally stable phase which can deteriorate due to the effects of neutral injection but which does not directly depend on the presence or density of energetic ions and which may also be independent of plasma rotation. This preliminary conclusion is supported by the observation that the particle confinement can obviously be regained during the injection pulse.

4.3 Recovery of particle confinement

The deterioration of particle confinement for the duration of the injection pulse does not seem to be an inevitable occurrence. There are cases where the particle confinement suddenly improves during the course of neutral injection after the usual deterioration.

In the following, two types of discharges are compared, one with the particle confinement reduced shortly after initiation of neutral injection (L(=low)-type) and another, where it is regained (H(=high)-type). The salient features and the major differences of the two discharge types are exemplified by the discharges #48o3 and 48o4. #48o3 is an L-type, #48o4 is an H-type discharge. There was no change in the setting of the external parameters of the machine or the injection system between the two discharges. The plasma current was 32o kA and the injection power 2.5 MW.

There is also no obvious difference in the plasma characteristics of the two discharges just prior to neutral injection. The transition occurred spontaneously again indicating that the state of the plasma seems to be close to the transition between two operational regimes.

Despite the spontaneous nature of and the lack of operational control over the transition, the two plasma regimes where investigated in detail during several series of discharges on different days. For cases where information is missing from the discharges #48o3 and 48o4, respectively, it is taken from these subsequent investigations.

The improvement in particle confinement time is documented most clearly by a sudden increase in plasma density after it has first decreased with neutral injection. The density variation for the two cases (L) and (H) is plotted in Fig.7a measured along the trace $z = a/2$. (The central trace was disturbed by electrical interferences with the neutral injector in the two cases. Central density values, however, could be measured during the series investigation.) During discharge (L) the density decreases as usual at constant external gas flux; in discharge (H) the density increases, as indicated by the arrow, without external intervention in particular, the external gas flux was held constant. The density increases even above the value before injection possibly because of the additional particle source of the beam.(The fluctuations on the density trace which show up on many other signals too will be discussed in chapter 6.) In the case where the density is kept constant by a feedback system, the external gas flux Φ_G is reduced at the moment the confinement improves. Figure 7b shows the feedback controlled density together with the external gas flux.

The density increase is not predominantly caused by an enhanced impurity influx into the plasma. Figures 8a and b show experimental results to document this. Together with the line density, which is replotted for orientation, the bolometrically measured plasma radiation and (Fig.8b) the spectroscopically measured radiation of OVI and FeXVI are plotted versus time. All radiation signals are divided by the electron line density and plotted for the two discharge types (solid line: type (H); dashed line: type (L)). During most of the injection phase the impurity signals for the high density case are lower than those for case (L) with low density. Thus, the density increase is not due to an increased impurity influx. This supports the contention that particle confinement is spontaneously improved.

As a result of the improved confinement the particle content increases with constant gas flux, and equally important, the wall-load is lower, because of the improved particle confinement, resulting in a cleaner plasma. The increase in FeXVI radiation and bolometer signal toward the end of neutral injection could be indicative of impurity accumulation in the plasma center a corollary of the improved confinement. (For comparison, see the soft X-ray radiation plotted in Fig.12a).

Other experimental observations provide evidence for an improvement in particle confinement. Together with the plasma density, Fig.9 shows the H_α/D_α-intensity measured far from the injectors together with the perpendicular charge exchange deuterium flux at an energy 1.13 keV (also measured far from each injector). At the moment the density starts to increase in case (H), the H_α/D_α-intensity and the charge exchange flux decrease, indicating a reduced recycling at the wall and consequently a lower

neutral density within the plasma at the positon of the diagnostic device. The particle pressure measured by an ionization gauge close to the vessel wall decreases to correspondingly lower values. The drop in charge exchange flux also indicates that the particle source term (see expression (9)) within the separatrix decreases.

Apart from the local recycling within the divertor chamber, measurements in the divertor are particularly sensitive to particle influxes and therefore sensitive to all questions related to particle confinement within the main plasma. Figure 1oa shows the H_α/D_α-intensity measured within the divertor chamber for the two cases. At the moment the confinement improves the H_α/D_α-intensity decreases to the value of the ohmic heating phase. As the change in H_α-radiation could also be caused by a different electron energy flux into the divertor chamber charge exchange measurements are performed there. Figure 1ob shows the atom flux which emerges from the neutralizer plate. According to their energy, the ions emerge from the main plasma and are not created by ionization within the boundary layer. The comparison between the two discharge types as documented by the results plotted in Fig.1oa and b demonstrates the reduced ion outflux from the main plasma into the boundary layer for discharge (H).

Though the boundary layer density as measured in the divertor chamber may be partly determined by the local recycling within the divertor chamber, it clearly shows the reduction of particle outflux from the main plasma into the boundary layer. Figure 11 shows the main plasma density together with the boundary layer line density measured by the outer channel in the upper divertor. At the moment of confinement improvement, the boundary

layer density decreases and shows a minimum. No such behaviour is observed in the boundary density of case (L). The formation of a minimum is reminiscent of the maximum in the boundary layer density (see Fig.2b) which appears when confinement deteriorates. The observation of a minimum can be understood qualitatively by the same arguments put forward in chapter 4.1.

As observed with the confinement of thermal particles, the confinement of runaway electrons also improves at the transition into the H-phase. This is documented by Fig. 12 which shows the hard X-ray flux of a discharge which made the transition from the L-phase into the H-phase shortly after the beginning of NI, when some runaway electrons were still confined. The hard X-ray flux decreases in the H-phase, nearly to its value during the ohmic phase. At bursts, additional runaway electrons are lost.

The relative contributions of particle confinement on one hand, and recycling and refuelling on the other, to the density variations of L- and H-type discharges may be estimated from the results plotted in Fig. 13. Plotted are density $\bar{n}_e$, external gas flux Φ_G, and as a reference to particle confinement, the backscattered atom flux from the neutralizer plate. The discharges #6028 and #5991 are nearly identical apart from a slight increase in injection power from 1.6 MW, which resulted in an L-type discharge (#6028), to 1.9 MW, which caused an H-type discharge (#5991). The slight <u>increase</u> in injection power should not cause an effective <u>reduction</u> in edge ion- and electron temperature which were necessary to increase the recycling coefficient and decrease the refuelling efficiency in order to give rise to the density increase. Therefore, the variation in density seems to be largely caused by changes in confinement properties of the plasma, and to a lesser extent, by modifications of plasma--wall interactions or of refuelling.

It is difficult to correlate the results presented up to now with MHD fluctuations as measured by soft X-ray diodes or Mirnov coils. Figure 14a shows the signal of a soft X-ray diode oriented toward the plasma center. With neutral injection, the signal increases, and has a spike at 1.46 sec caused by a sawtooth-relaxation which is followed by an unquiet phase which lasts till 1.51 sec. Thereafter, the diode signal continues to increase but it stays quiet without further fluctuations during discharge type (H). In contrast, it stays noisy till the end of injection during discharge type (L).

A similar behaviour is found in the Mirnov coil signal. With neutral injection the fluctuation level suddenly increases. Though discharge type (H) seems to be characterized by less fluctuations in soft X-ray diode as well as Mirnov coil signal one has to be cautious in correlating these findings with better confinement. The sudden increase in density in case (H) occurs during the noisy phase of the discharge as seen from both soft X-ray diode and Mirnov coil signal (see arrow in Fig. 14). Though there is no change in the level of fluctuations correlated with the sudden increase of density, the plasma develops thereafter with less MHD activity.

5. EFFECTS OF IMPROVED PARTICLE CONFINEMENT ON PLASMA PARAMETERS

The improved particle confinement has a strong and positive impact on plasma parameters which develop after the transition into the regime with better confinement.This will be illustrated by two parameters which are particularly important for fusion devices - β_{pol} and the neutron counting rate.

The vertical field current necessary to stabilize the plasma column and the radial plasma position are plotted in Fig. 15 for the two discharge types. As a result of the beam parallel momentum the plasma column expands radially by ~2 cm during the first 3o msec after initiation of the beams. An increase in the vertical field then restores the original plasma position approximately. In case (L) a higher but stationary vertical field current is required to keep the plasma at its original location (apart from an off-set in plasma position which is inherent to the feedback system). From the Shafranov relation, $\beta_p + l_i/2 = 1.63$ is deduced.

Case (H) shows a different and promising behavior. At the instant the particle confinement is restored and the density starts to increase the plasma column expands again. The vertical field current increases in order to maintain the plasma position. A high value of $\beta_p + l_i/2 = 2.2$ results at a plasma current of 32o kA. Within reasonable limits of $l_i/2$, β_p is estimated: $1.55 \leq \beta_p \leq 1.75$. This value corresponds to about 4o % of the aspect ratio.

Another important aspect is the thermo-nuclear neutron flux $\dot{N}_n$ during the auxiliary heating phase. As documented by Fig. 16, $\dot{N}_n$ rises during neutral injection but in case (H) it starts to increase again as soon as confinement improves and reaches 3 times the value of the standard, low-confinement discharge.

6. FLUCTUATIONS DURING THE HIGH-β_p PHASE

During the high β_p-phase of discharge type (H) periodic fluctuations occur which are obvious from the traces plotted in Figs. 7 to 16. These fluctuations, which occur as bursts in the Mirnov coil signals, have several consequences on the particle confinement. At the instant of a burst, the confinement within the outer plasma zones deteriorates causing density and electron temperature to decrease there. As documented by Fig.9 such a decrease in density is accompanied by a peak in H_α/D_α-intensity in the main plasma volume and (see Fig.10a) the divertor. Figure 17a shows the radial plasma position (dashed curve) and the line average density along the chord $z = a/2$ - both with fluctuations; Figure 17b shows the electron temperature as measured by electron cyclotron emission from $r = 22$ cm and for comparison in Fig. 17c from $r = 3$ cm. (The deep minima at $t = 1.52$ sec is caused by a chopper to monitor the signal base line). Though these fluctuations resemble ordinary sawteeth oscillations they do not appear in the plasma center but in the outer plasma zones. This is clearly seen from the electron temperature fluctuations (comparison of Figs.17b with 17c) but also from the soft X-ray signal as plotted in Fig.14a (solid line), which emerges predominantly from the plasma center and which shows no oscillations of the type measured by the Mirnov coils (Fig.14b). Furthermore, the FeXVI-radiation originating more from the plasma center shows weak or no oscillations contrary to the OVI-radiation which is located at the plasma edge and therefore fluctuates strongly. (The fluctuations are not caused by dividing the signal by the density. The original OVI-radiation is also modulated.)

The sudden loss of plasma pressure causes a disturbance in the positional equilibrium of the plasma column. At the given vertical field the plasma column shrinks in larger radius

typically by 0.6 cm. Because the plasma column is transiently stabilized by mirror currents in the plasma vessel during this phase, an estimate of the loss in β_p from the shift in plasma position is not possible. During the quiescent phase between two bursts, T_e and n_e increase again and the high β_p-value is regained.

The fact that plasma ions during this phase can reach the vessel wall surrounding the main plasma to recycle there and cause fluctuations in the H_α/D_α-intensity indicates a long density fall-off length of the boundary layer plasma. Measuring the spatial profile of ions being neutralized at and back-reflected from the neutralizer plate is a method to estimate the fall-off length with the required time resolution. Figure 18a shows the charge exchange flux emitted approximately at the peak of the backscattering intensity profile at the plate (note the insert for geometrical arrangement) and Fig.18b shows the flux 2.25 cm above from the separatrix. The intensity of back-scattered flux at this poisition is smaller than the flux emitted at the actual separatrix intersection but it is more strongly modulated. (These measurements are taken on a shot to shot basis. Therefore the frequency of the bursts shown in Fig.18a is different to the one in Fig. 18b) The comparison of Fig.18a and b immediately indicates that the fall-off length increases during the bursts. Figure 19 shows the spatial variation of the backscattered flux intensity during the ohmic phase between two bursts and at a burst. The decay length is 0.68 cm in the ohmic phase and increases slightly during NI to 0.75 cm between the bursts. At a burst, however, the decay length increases to at least 2.1 cm. As the density profile of the boundary layer is determined by the competing processes of parallel flow and perpendicular diffusion, an increase of the diffusion

coefficient by about an order of magnitude is required to explain the increase in density fall-off length. The actual increase in fall-off length and perpendicular transport coefficient could be more because the time resolution of the charge exchange flux detection system may be insufficient to measure the full amplitude of the particle bursts.

It is not clear at present what mechanism causes these gross instabilities which give rise to a loss in confinement and to a limitation in β_p. It is particularly not clear whether the plasma jumps periodically between the two possible states - the high-β_p state between the bursts and the low-β_p state as usually encountered thereby causing the bursts.

7. CONCLUSIONS

The decrease in plasma density which is generally observed during neutral injection into ASDEX divertor plasmas is analyzed. There are experimental indications, that the density decrease is partly caused by a reduction in recycling coefficient and refueling efficiency. Measurements of the boundary layer line density, H_α/D_α-intensity around the torus and hard X-ray radiation from runaway electrons also indicate that a reduction in particle confinement occurs with neutral injection which results in reduced plasma density at constant fueling rate. There is no clear correlation between reduction in particle confinement and the presence of energetic beam ions, a possible plasma rotation, or MHD-activity. It seems most probable, that the deterioration in particle confinement is caused by unfavorable profile changes in the beam heated plasma which cause a transition into a low confinement regime.

There are cases - observed rather frequently - where the plasma changes spontaneously into a state of higher particle confinement in the course of neutral injection after first decreasing in the usual manner. In this regime the plasma density rises, the β_p-values correspond to 4o % of the aspect ratio and a high neutron flux develops. This high β_p-regime is characterized by frequent bursts in the Mirnov coil signal which cause transient reductions in the particle and energy density of the outer plasma layers.

ACKNOWLEDGEMENT

The efforts of the ASDEX operational team and the neutral injection operational group are acknowledged. Thanks are due to Mrs.H.Volkenandt and Mrs.S.Beutler for their patience in preparing the drawings and the manuscript.

REFERENCES

/1/ D.Swain et al., Proc.9th Europ. Conf. on Contr. Fusion and Plasma Phys., Oxford (1979).

/2/ K.B.Axon et al., Proc. 8th Int.Conf.on Plasma Physics and Contr.Nucl.Fus.Research,Vol.1, IAEA, Vienna (1981) p.413.

/3/ H.C.Howe, Jour.of Nucl. Mat. 93 & 94 (198o) 17.

/4/ F.Wagner et al., Proc.3rd Joint Varenna-Grenoble Int. Symp. on Heating in Tor.Plasmas, Grenoble (1982).

/5/ F.Wagner, Investigation of Limiter Recycling in the Divertor Tokamak ASDEX, IPP-Report III/71, Garching (1981).

/6/ The ASDEX-Team, Proc. IAEA Techn. Comm. Meeting on Divertors and Impurity Control, Garching (1981) p.4o.

/7/ H.M.Mayer et al., Proc.5th Int. Conf. on Plasma Surface Inter.inContr. Fusion Devices, Gatlinburg(1982).

/8/ R.L.Freeman and E.M.Jones, CLM-R-Report 137, Culham (1974).

/9/ K.Büchl and G. Vlases, private communication.

FIGURE CAPTIONS

Fig. 1: Time dependence of the line average density measured through the plasma center. The neutral injection phase is marked as in the following plots by a hatched area; it is terminated at arrow 1. At arrow 2 the density feedback system is activated to restore the original density.

Fig. 2a: Line density versus time measured along three horizontal chords with different distances from the plasma center.

Fig. 2b: Line density of the outer boundary plasma measured in the lower divertor chamber.

The dashed curves are the calculated quantities as described in the text.

Fig. 3: Time variation of line average plasma density ($z = 0$) together with the $H\alpha/D\alpha$-intensity (the sensor measures the sum of $H\alpha$- and $D\alpha$intensities) measured at two different toroidal positions far from the neutral injector.

Fig. 4: Plotted are plasma current I_p, line average density $\bar{n}_e$ ($z = 0$) and hard X-ray counting rate $\dot{N}_x$ through three phases of the discharge: The initial phase, the neutral injection phase with expanded time scale and the termination of the discharge.

Fig. 5: Time dependence of the line average density $\bar{n}_e$ measured along the chords $z = 0$ (plasma center) and $z = a/2$, the $H\alpha/D\alpha$-intensity in the main plasma chamber far away from the injectors and the hard X-ray radiation N_x.

Fig. 6: Time dependence of the line average density along the chord $Z = a/2$ for three different injection powers: ——— 0.6 MW, ---- 1.2 MW and .... 2.6 MW.

Fig. 7a: Line average density $\bar{n}_e$ along the chord $z = a/2$ of the two discharge types H (solid line) and L (dashed line). The density is not feedback controlled but kept constant during the neutral injection phase. The arrow indicates the transition to improved confinement in this and the following figures.

Fig. 7b: Line average density $\bar{n}_e$ and external gas flux Φ_G during neutral injection with a feedback controlled density. At the transition to improved confinement (arrow) Φ_G decreases.

Fig. 8a: Plasma radiation from the two discharge types as measured by a bolometer. The signal is divided by the plasma density. The line average density is replotted for reference.

Fig. 8b: Radiation of OVI and FeXVI each normalized against plasma density from the two discharge types.

Fig. 9: H_α/D_α-intensity and the charge exchange flux measured in the main plasma chamber at a position far away from the injectors. Energy of the charge exchange atoms $E = 1.13$ keV.

Fig.1oa: H_α/D_α-intensity and
Fig.1ob: atom flux backscattered from the neutralizer plate measured in the upper divertor chamber. Energy of the backscattered atoms $E = 374$ eV.

Fig.11: Line average plasma density $\bar{n}_e$ ($z = a/2$) (for reference) and line density of the outer boundary layer measured in the upper divertor channel.

Fig.12: Line density $\bar{n}_e$ and hard X-ray flux at the transition from L-type to H-type discharge (indicated by a dashed line).

Fig.13: Line density (a), external gas flux Φ_G (b) and reflected atom flux Φ_G from the neutralizer plate (c) for an L-type (#6028) and an H-type (#5991) discharge.

Fig. 14a: Soft X-ray radiation measured by a pin-hole diode oriented to r = 2 cm of the two discharge types.

Fig. 14b: Fluctuations of $\dot{B}$ as measured by Mirnov coils of the two discharge types H and L. The arrow indicates the instant when the density starts to increase during discharge type (H).

Fig. 15: Vertical field current I_{VF} and shift of the plasma position $R-R_o$ ($R_o = 165$ cm) of the two discharge types.

Fig. 16: Neutron count rate of the two discharge types H (solid curve) and L (dashed curve).

Fig. 17a: Plasma density $\bar{n}_e$ and position $R-R_o$ during neutral injection together with

Fig. 17b: electron temperature measured at r = -22 cm and

Fig. 17c: electron temperature at r = 3 cm by electron cyclotron radiation. The minima at 1.52 sec in the T_e-traces are experimental. The signal is chopped to monitor the signal-offset.

Fig. 18: Flux of atoms backscattered from the neutralizer plate
a) at the intersection separatrix - neutralizer plate
b) 2.25 cm above the separatrix during discharge type H.
The inset shows the experimental geometry. The measurements are taken at two different shots, therefore the frequency of the bursts are different.

Fig. 19: Charge exchange flux backscattered from the neutralizer plate versus vertical distance from the intersection of separatrix with the neutralizer plate.
Plotted is the backscattering profile during the ohmic phase (.), during the neutral injection phase (o) and at a burst (x). The exponential decay length is indicated in the main text.

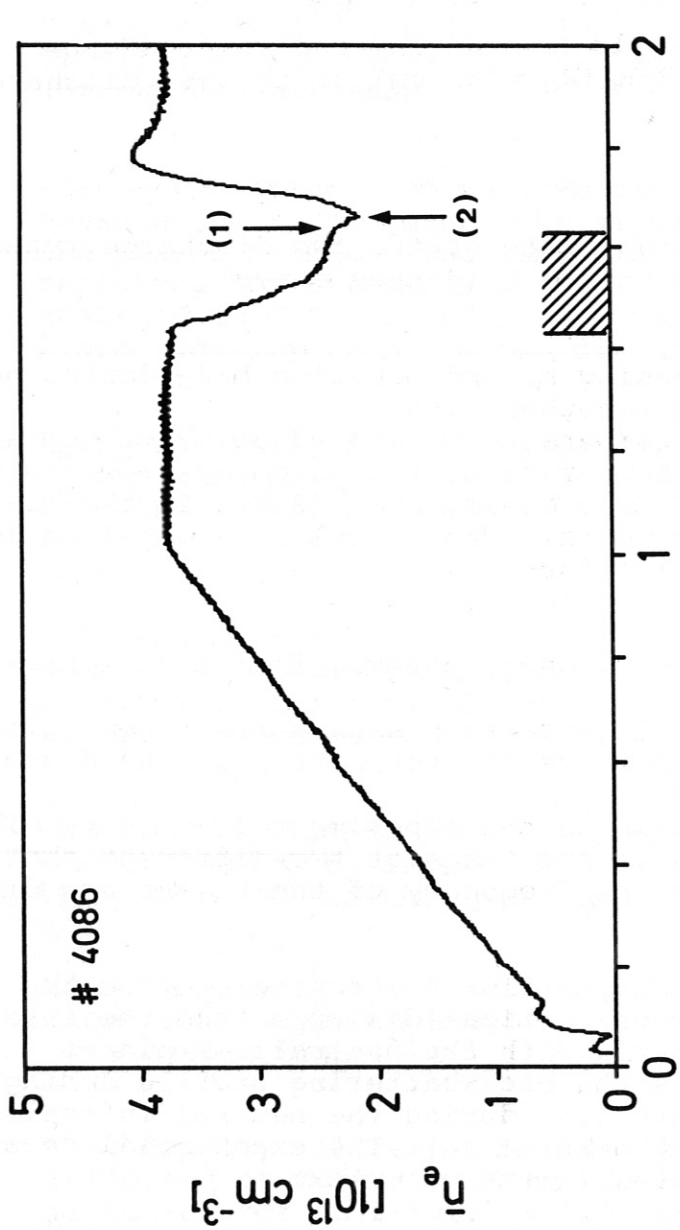

Fig.1

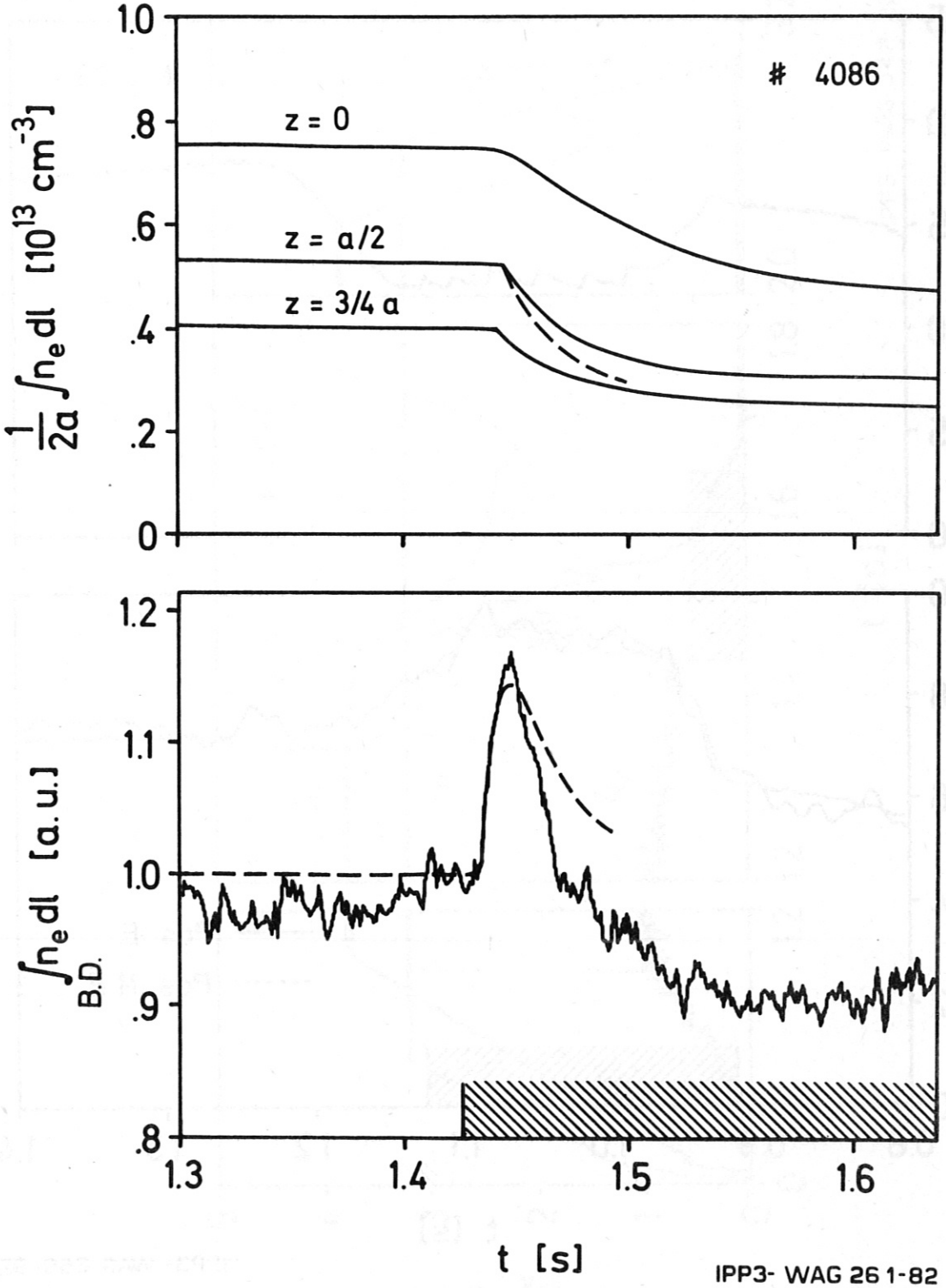
1.0
.8
.6
.4
.2
0
# 4086
z = 0
z = a/2
z = 3/4 a
$\frac{1}{2a}\int n_e dl$ [10^{13} cm^{-3}]
1.2
1.1
1.0
.9
.8
$\int n_e dl$ B.D. [a.u.]
1.3
1.4
1.5
1.6
t [s]
IPP3- WAG 26 1-82

Fig.2a

Fig.2b

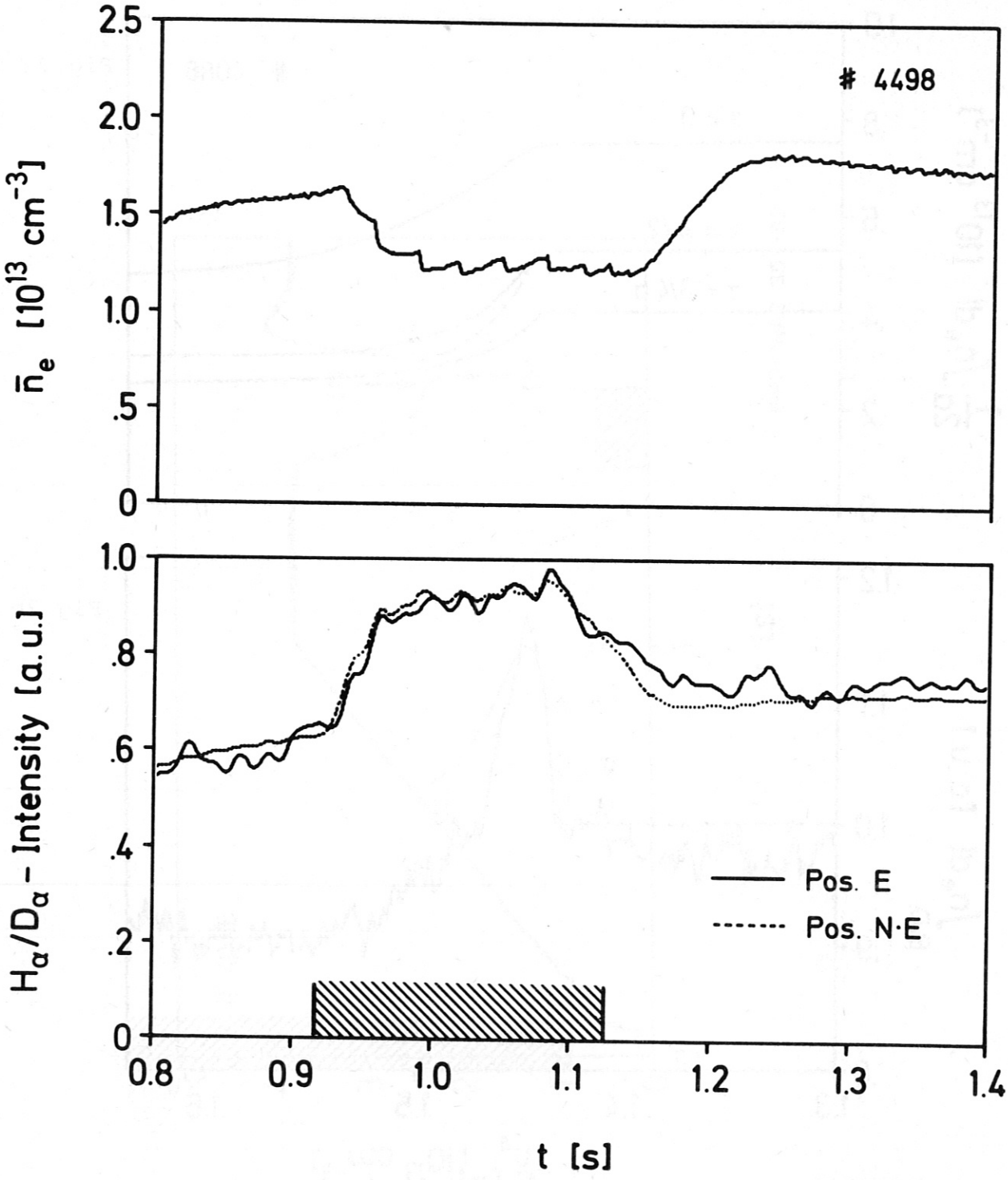

IPP3- WAG 259-82

Fig.3

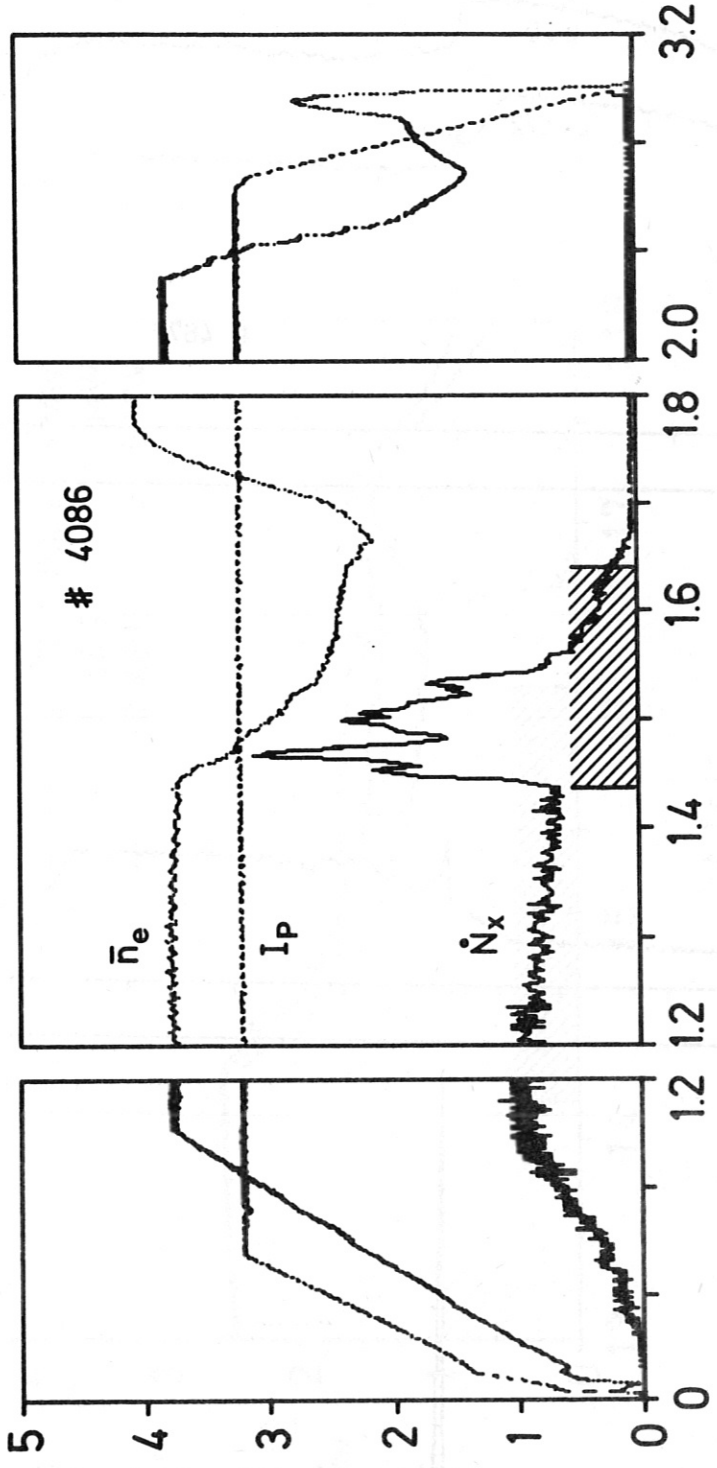
$\bar{n}_e$ [10^{13} cm^{-3}]
I_P [10^5 A]
$\dot{N}_x$ [a.u.]
4086
$\bar{n}_e$
I_P
$\dot{N}_x$
t [s]
IPP3- WAG 348-82

Fig.4

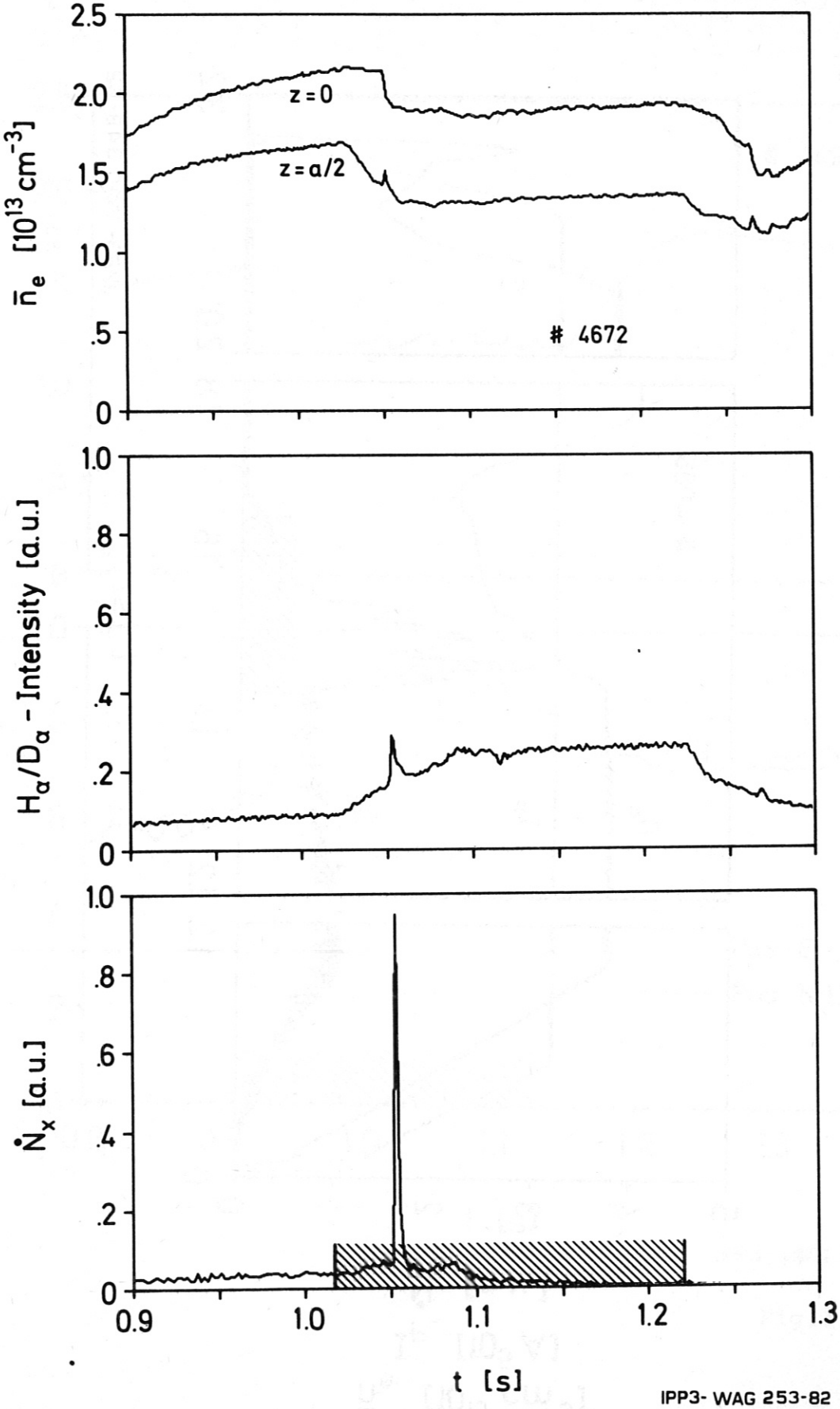
2.5
2.0
1.5
1.0
.5
0
$\bar{n}_e$ [10^{13} cm^{-3}]
z = 0
z = a/2
# 4672
1.0
.8
.6
.4
.2
0
H_α/D_α - Intensity [a.u.]
1.0
.8
.6
.4
.2
0
$\dot{N}_x$ [a.u.]
0.9
1.0
1.1
1.2
1.3
t [s]
IPP3- WAG 253-82

Fig.5

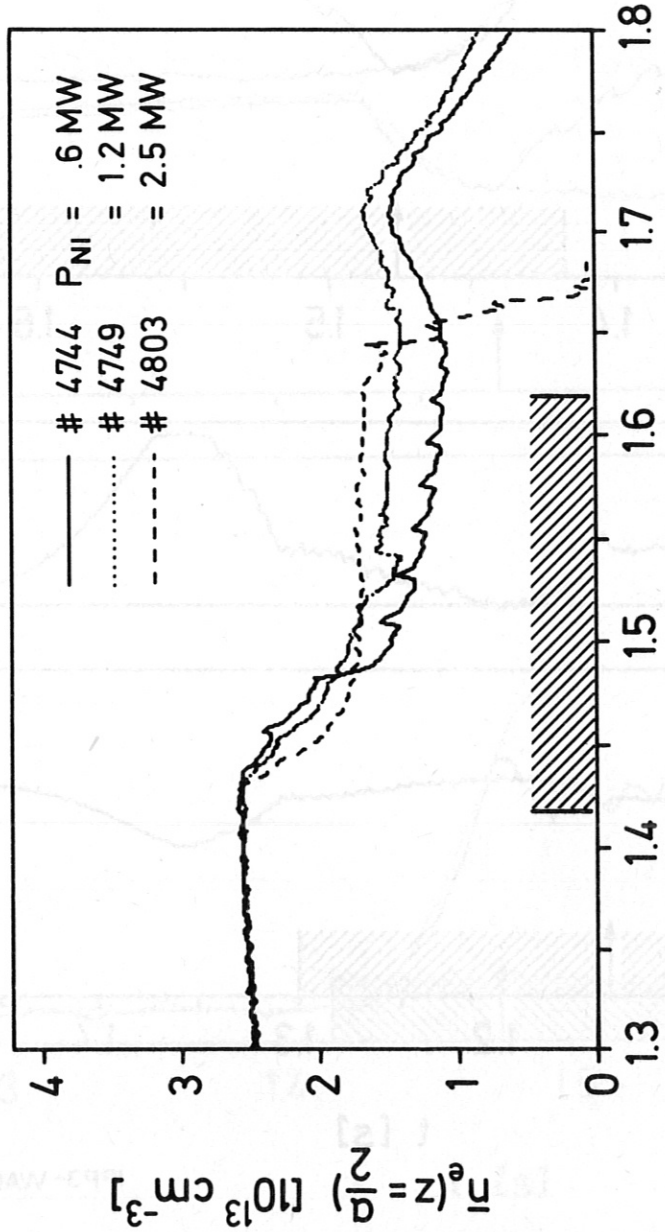

IPP3- WAG 352-82

Fig.6

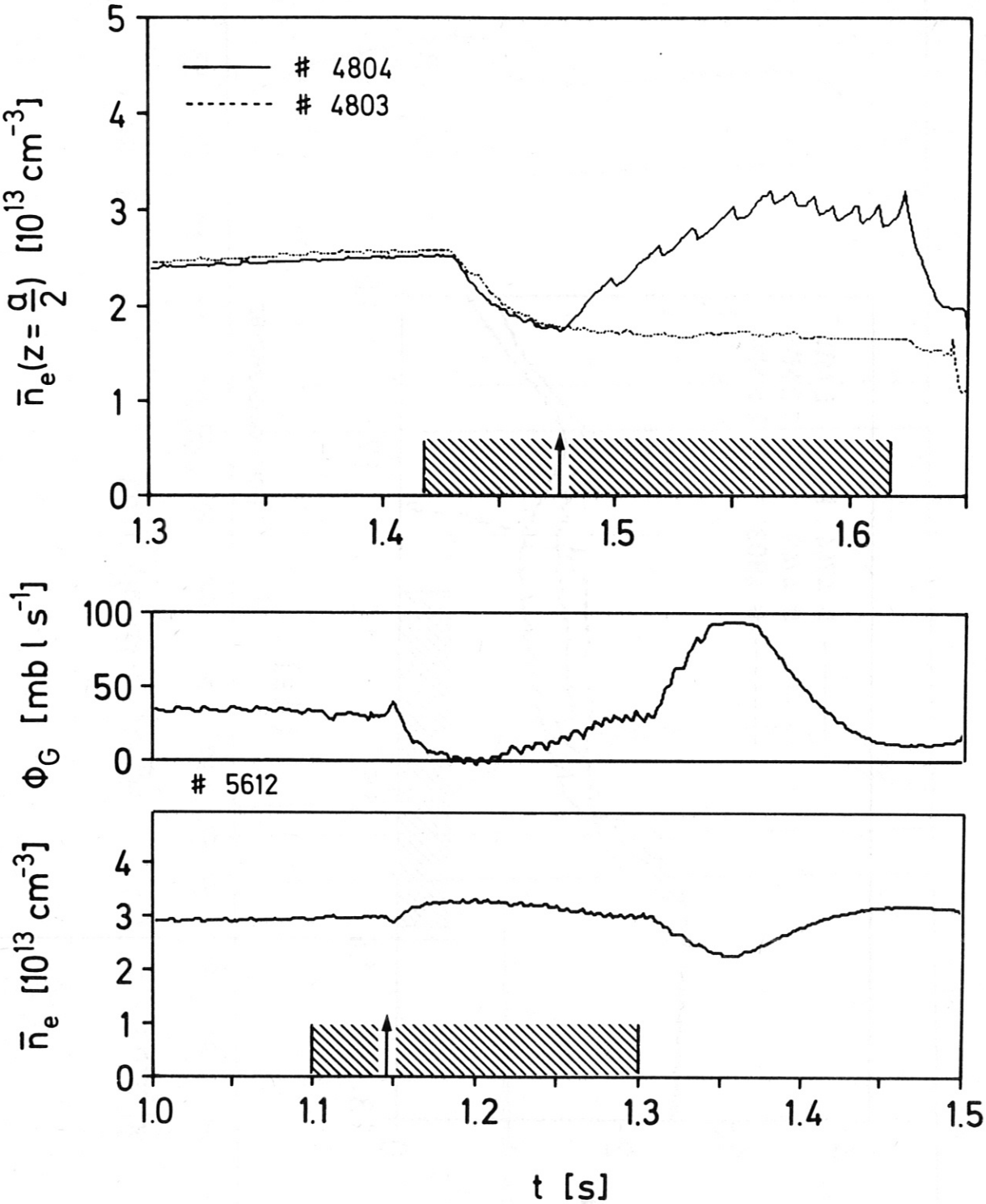

Fig.7a

Fig.7b

IPP3- WAG 34 1-82

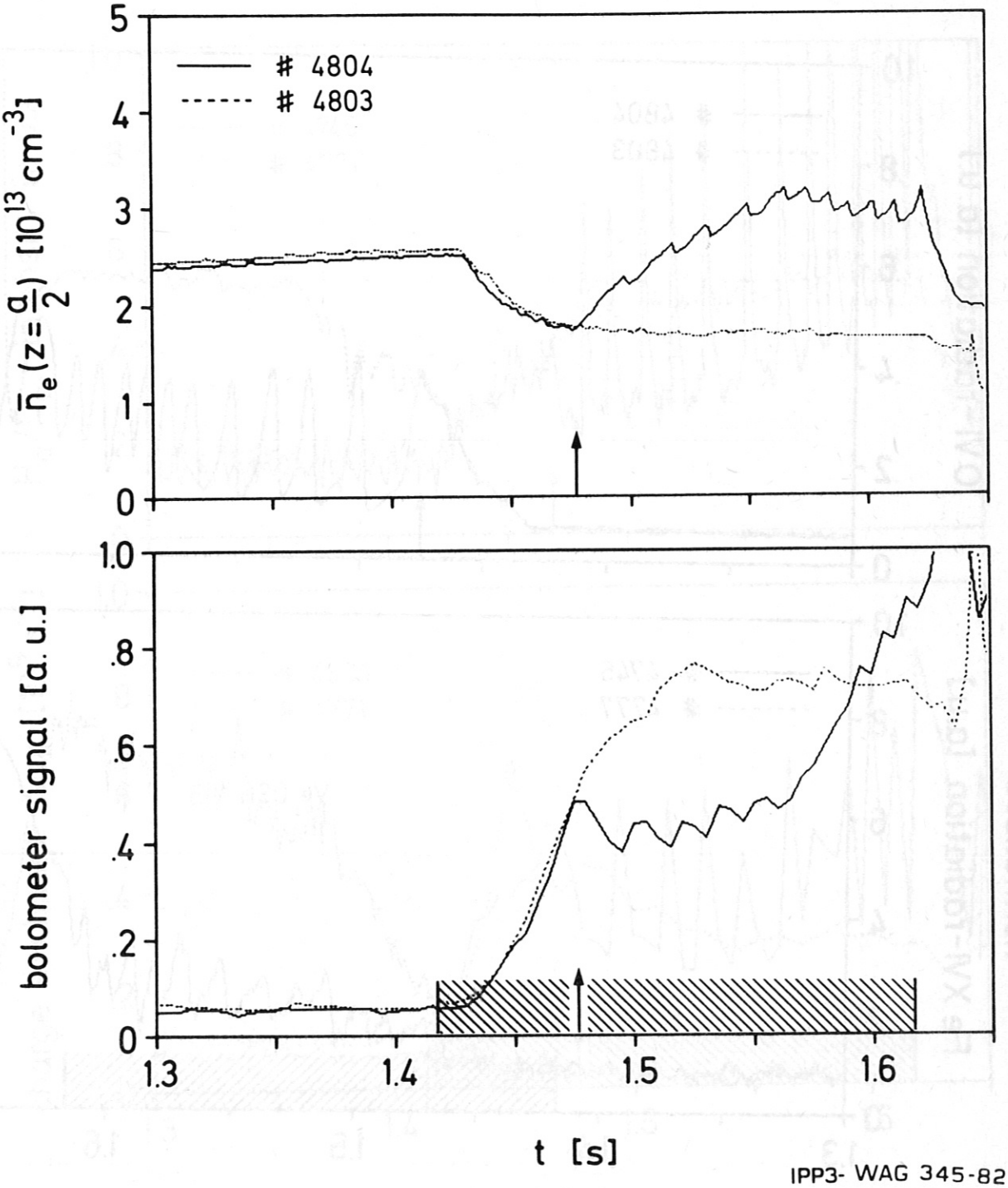

IPP3- WAG 345-82

Fig.8a

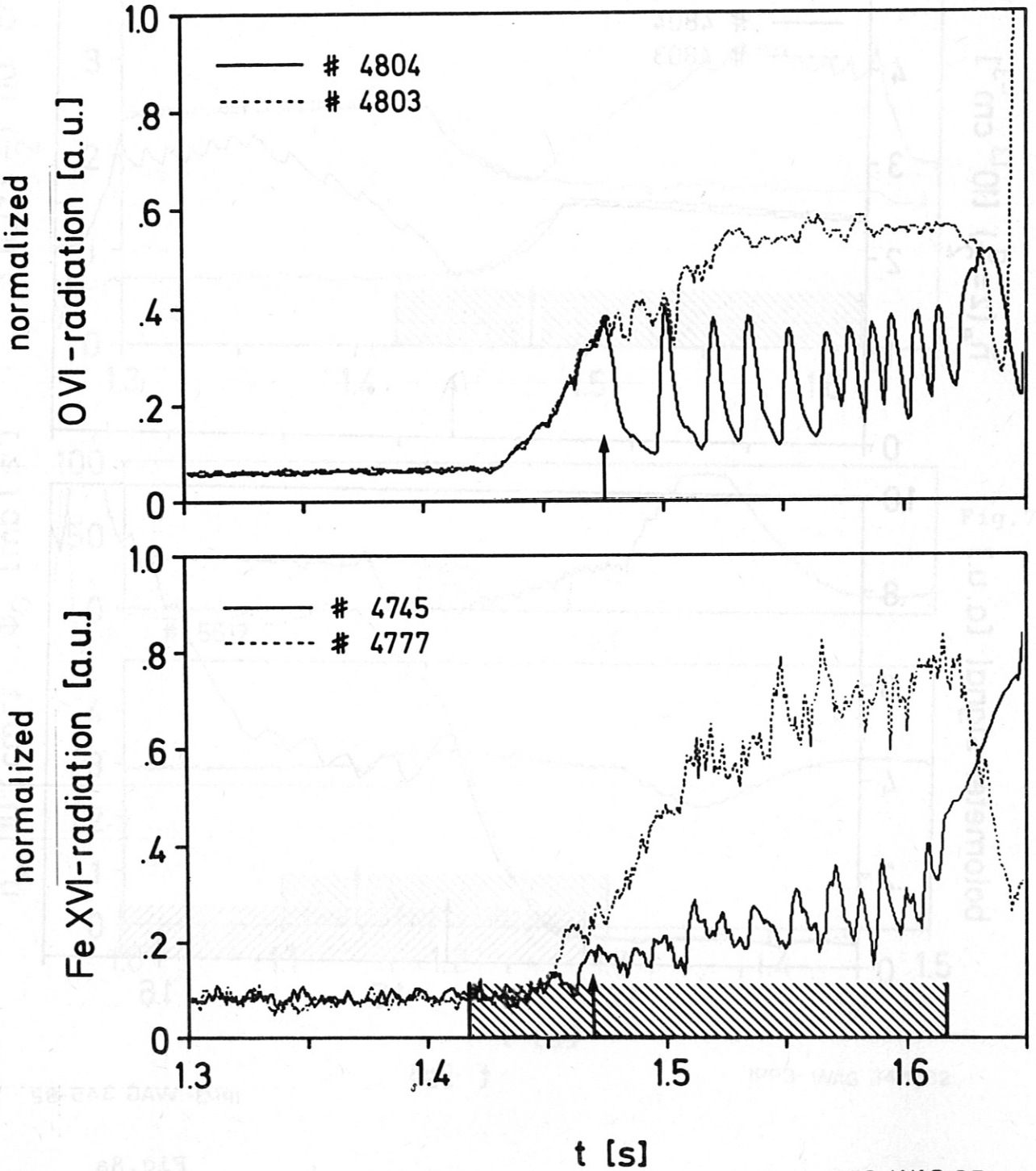

IPP3- WAG 254-82

Fig.8b

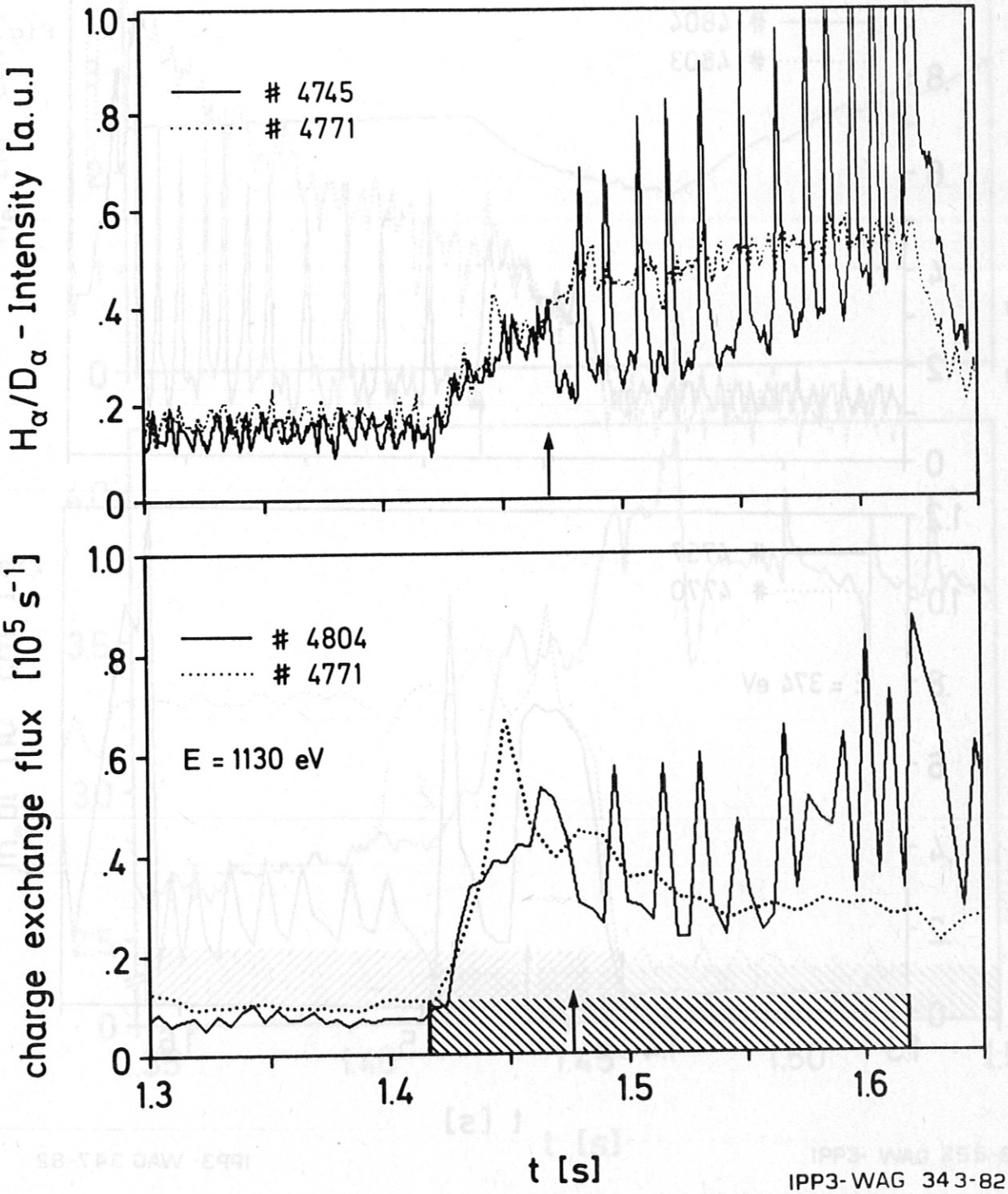
1.0
.8
.6
.4
.2
0
4745
4771
H_α/D_α - Intensity [a.u.]
# 4804
# 4771
E = 1130 eV
charge exchange flux [10^5 s^{-1}]
1.3
1.4
1.5
1.6
t [s]
IPP3-WAG 343-82

Fig.9

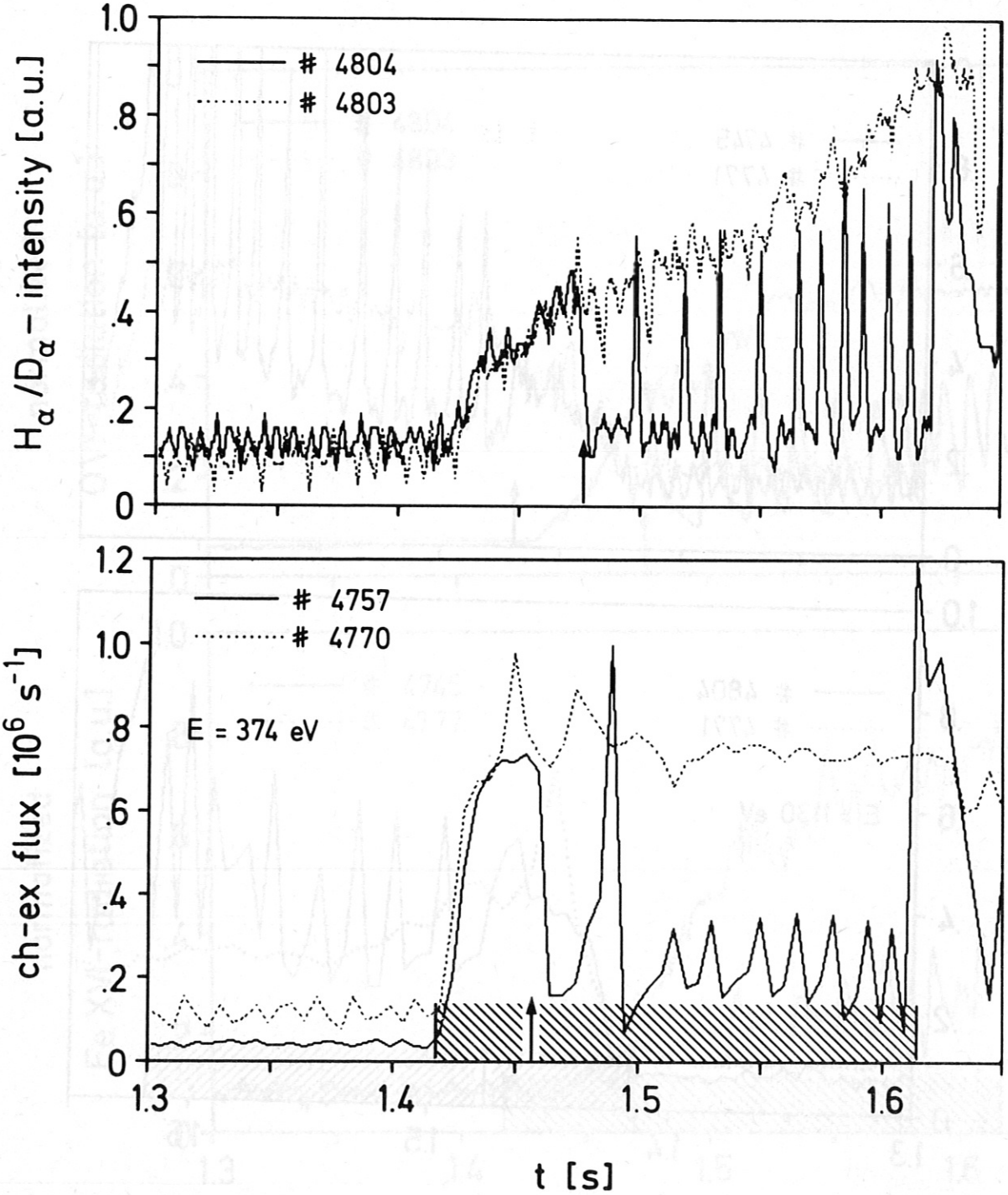

Fig.1oa

Fig.1ob

IPP3- WAG 347-82

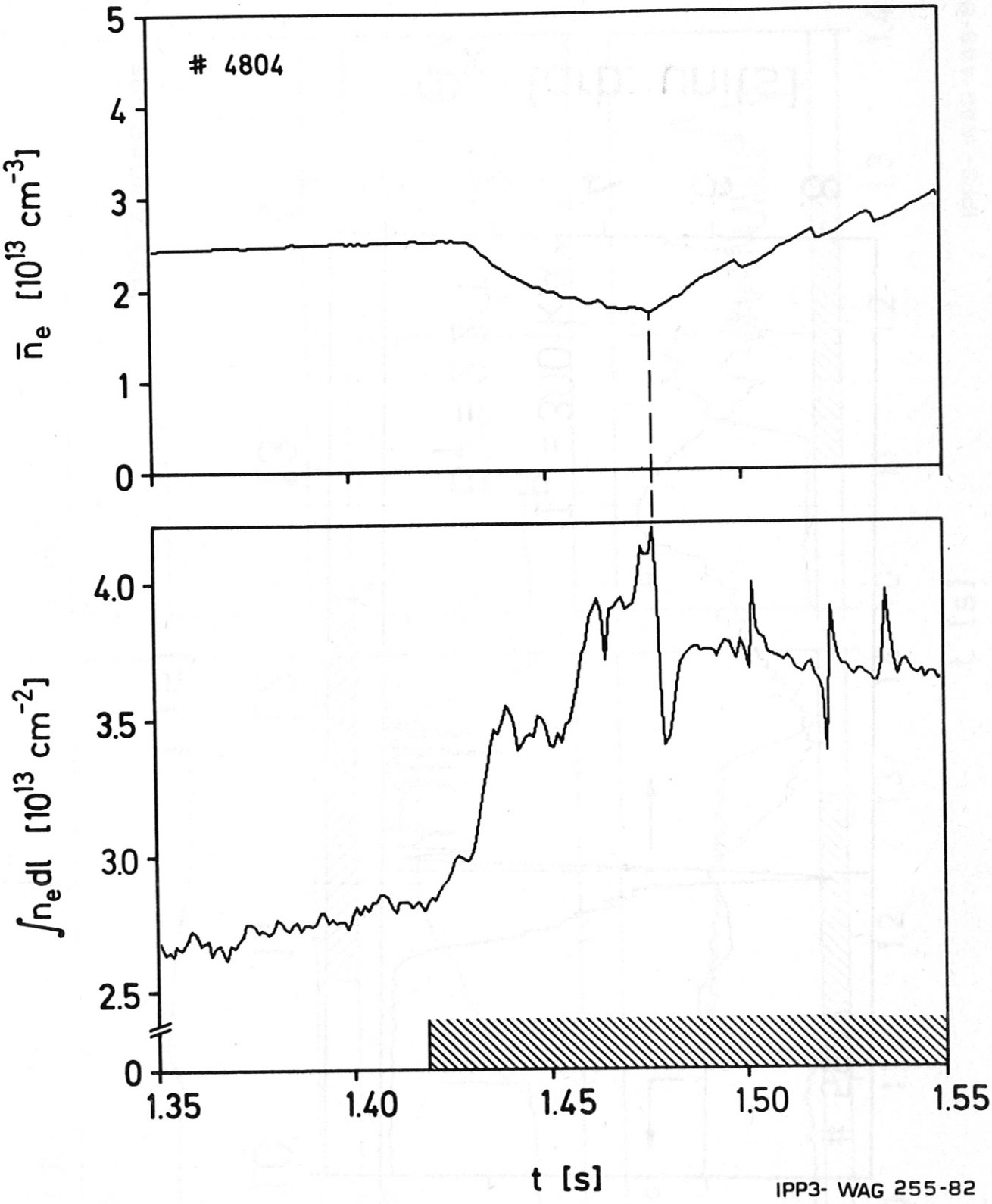

Fig.11

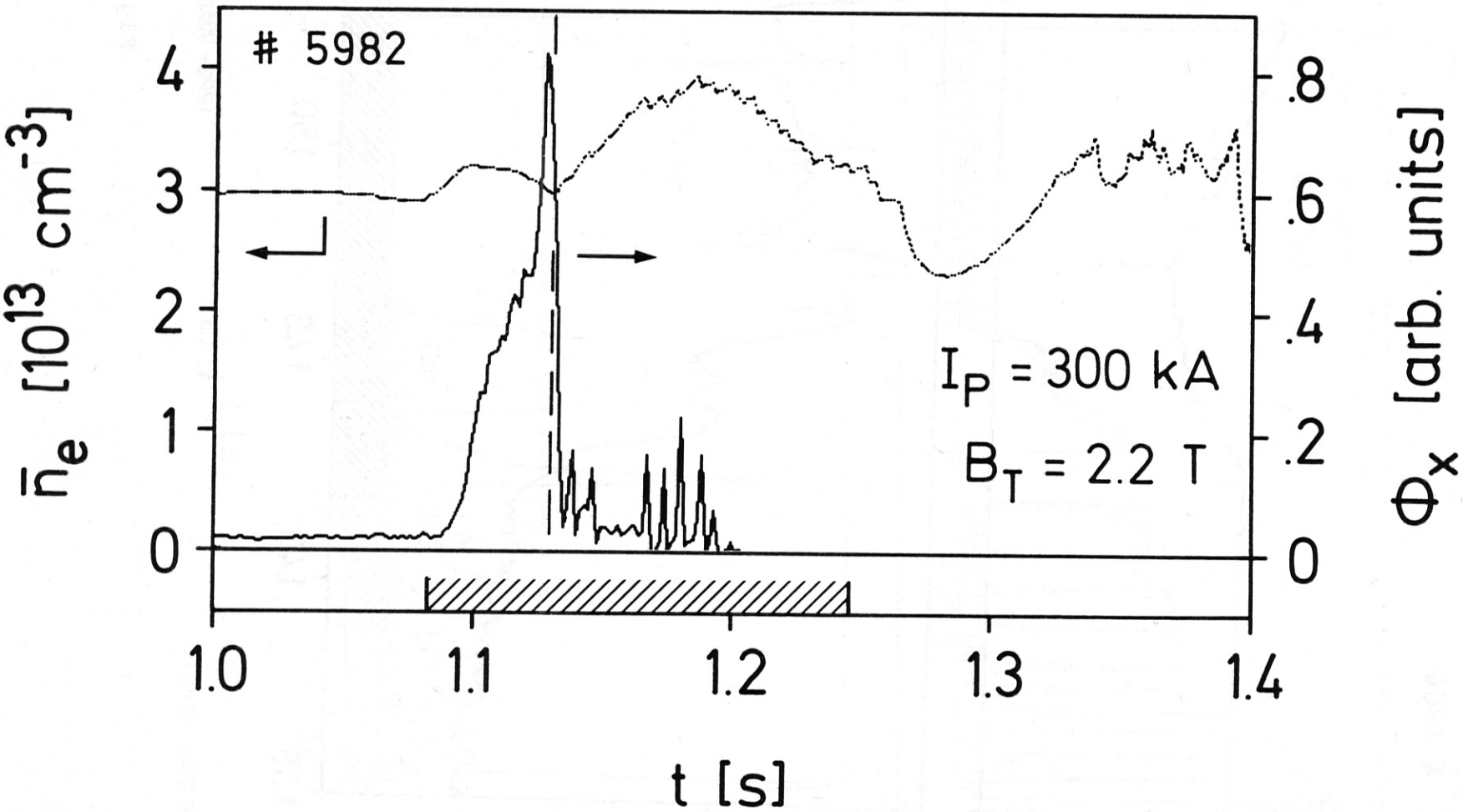

IPP3- WAG 451-82

Fig. 12

Fig. 13

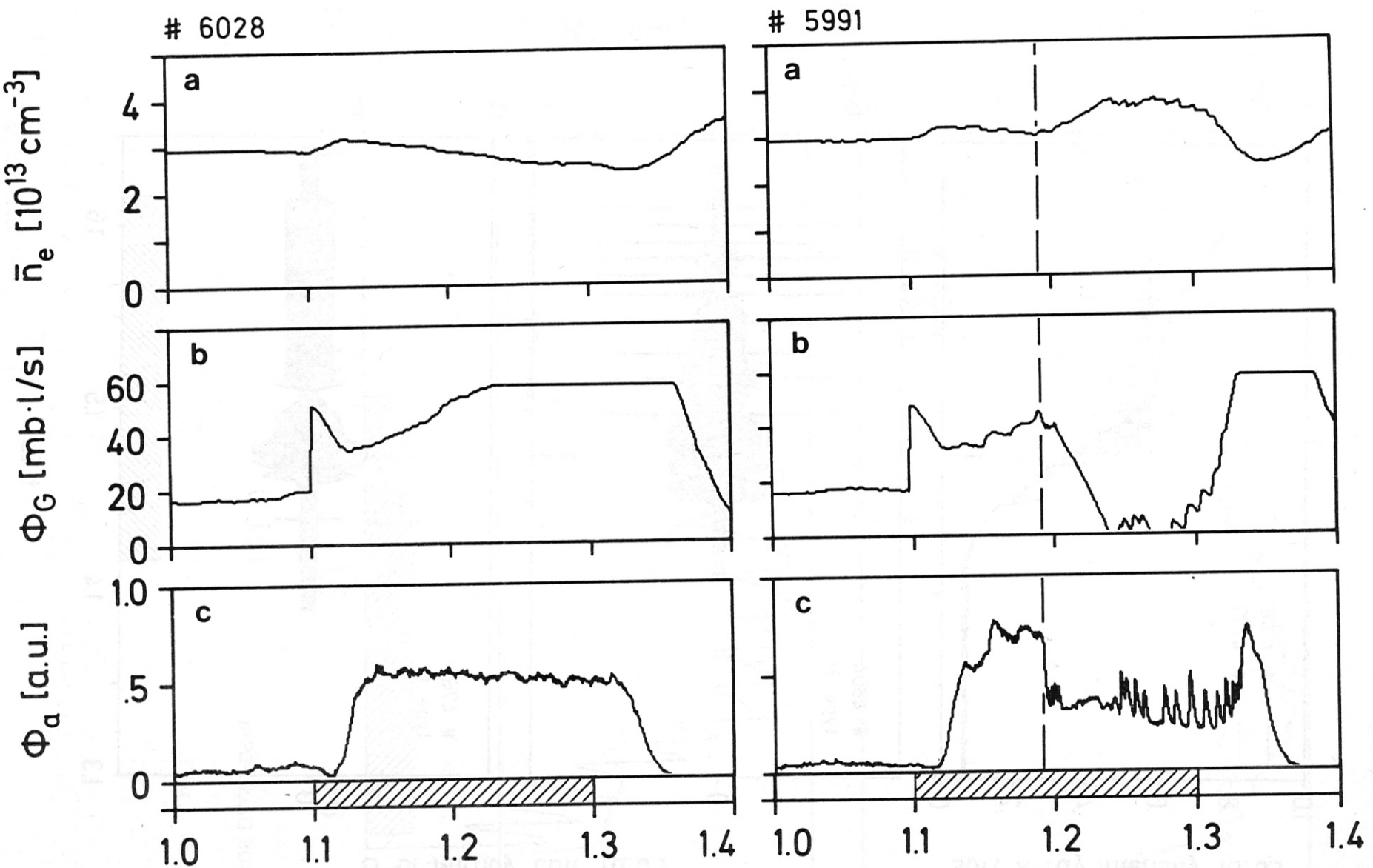
6028
5991
a
b
c
$\bar{n}_e$ [10^{13} cm^{-3}]
Φ_G [mb·l/s]
Φ_a [a.u.]
t [s]
IPP3- WAG 448-82

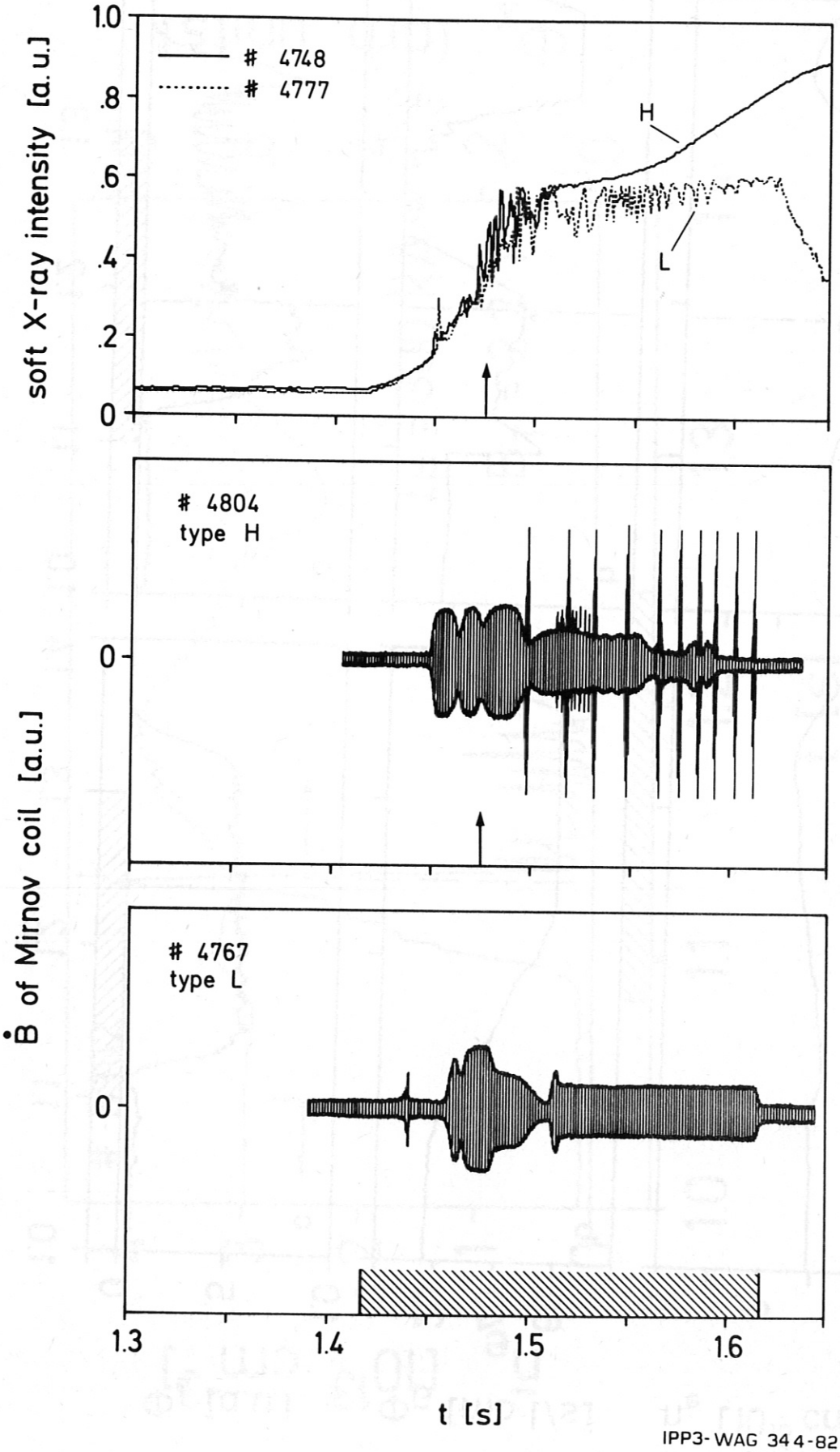

Fig. 14a

Fig. 14b

IPP3-WAG 344-82

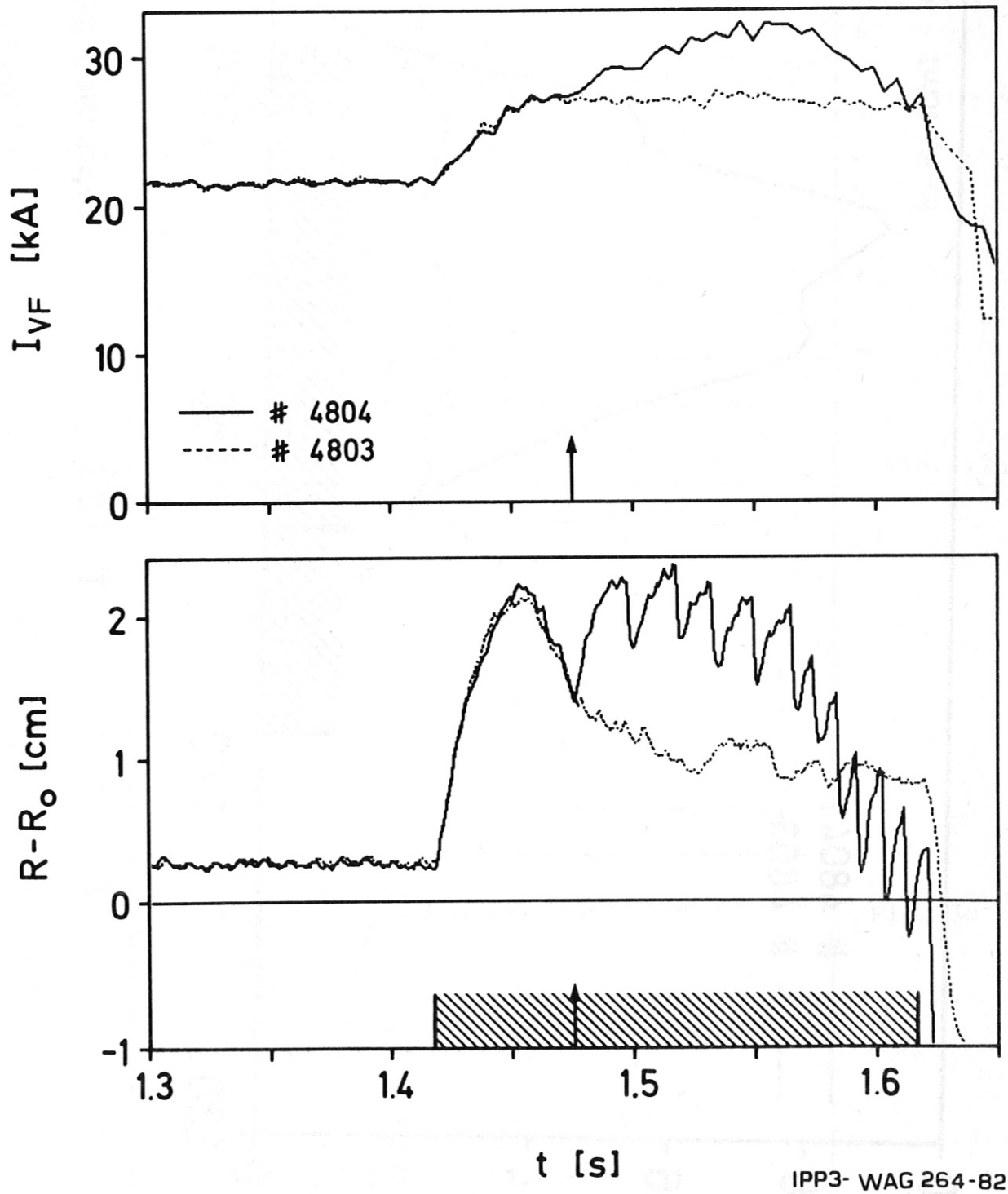
30
20
10
0
I_{VF} [kA]
4804
4803
2
1
0
-1
R-R_o [cm]
1.3
1.4
1.5
1.6
t [s]
IPP3- WAG 264-82

Fig. 15

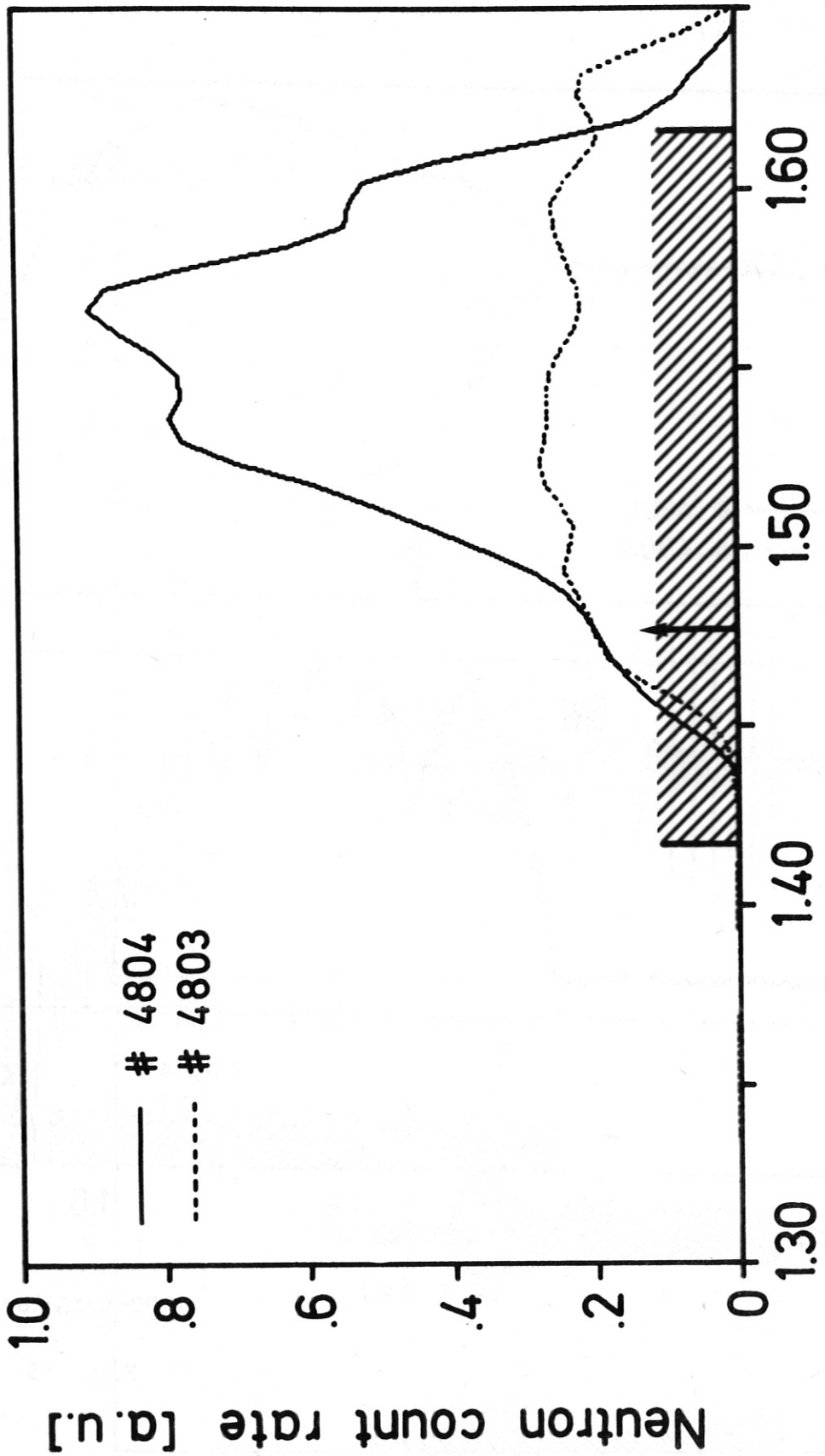
Neutron count rate [a.u.]
1.0
.8
.6
.4
.2
0
1.30
1.40
1.50
1.60
t [s]
4804
4803
IPP3-WAG 256-82

Fig. 16

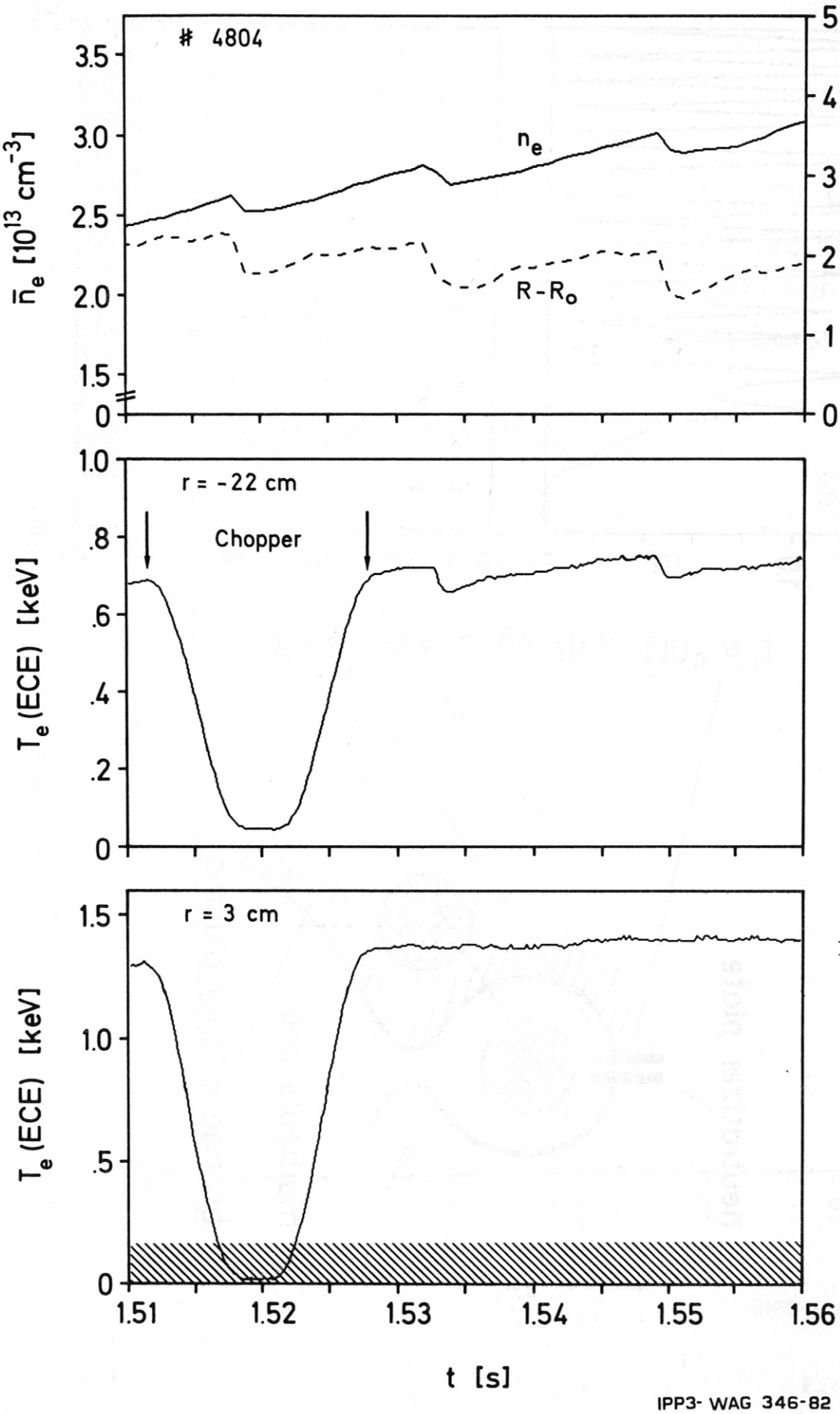

Fig. 17a

Fig. 17b

Fig.17c

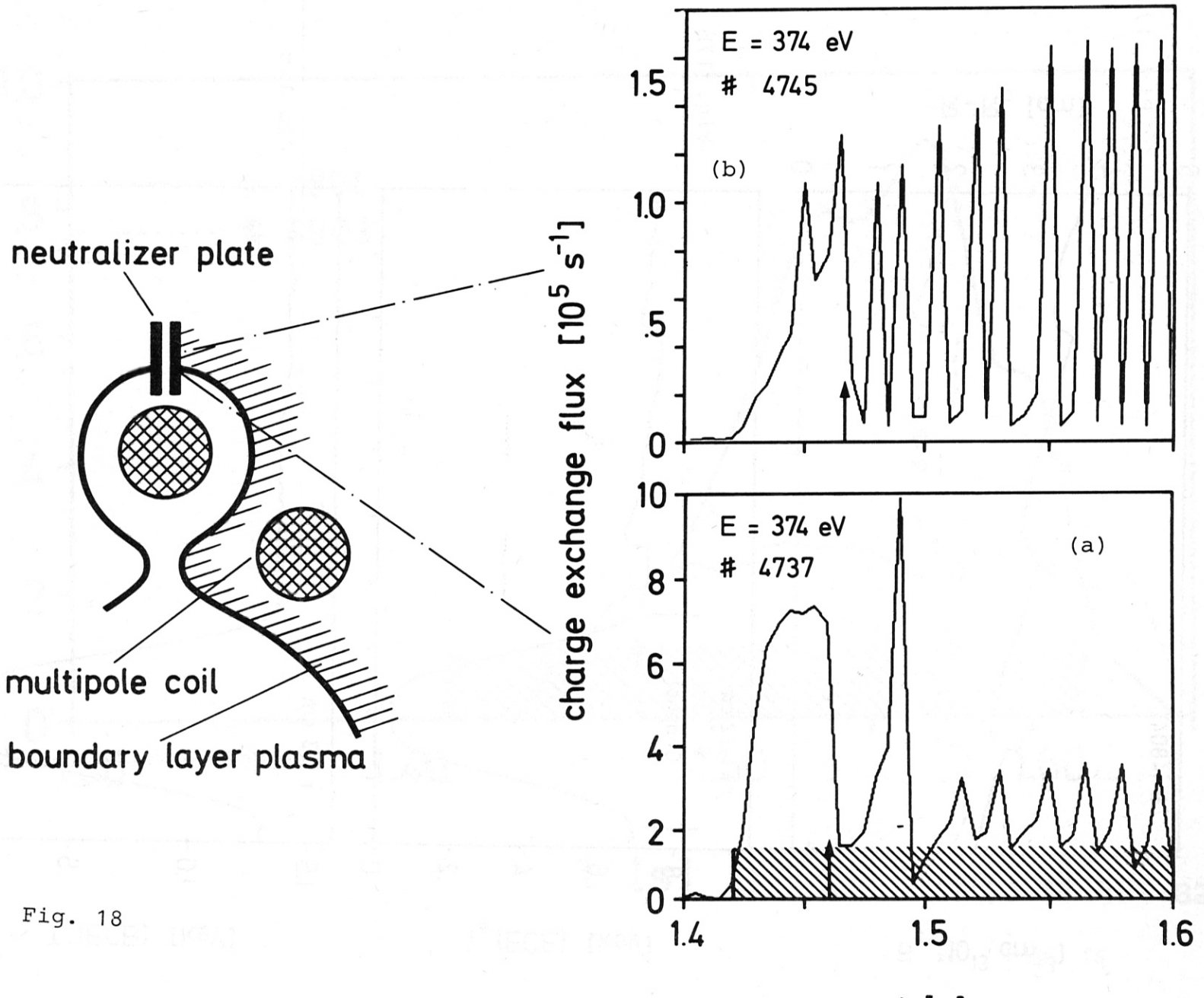

Fig. 18

IPP3- WAG 262-82

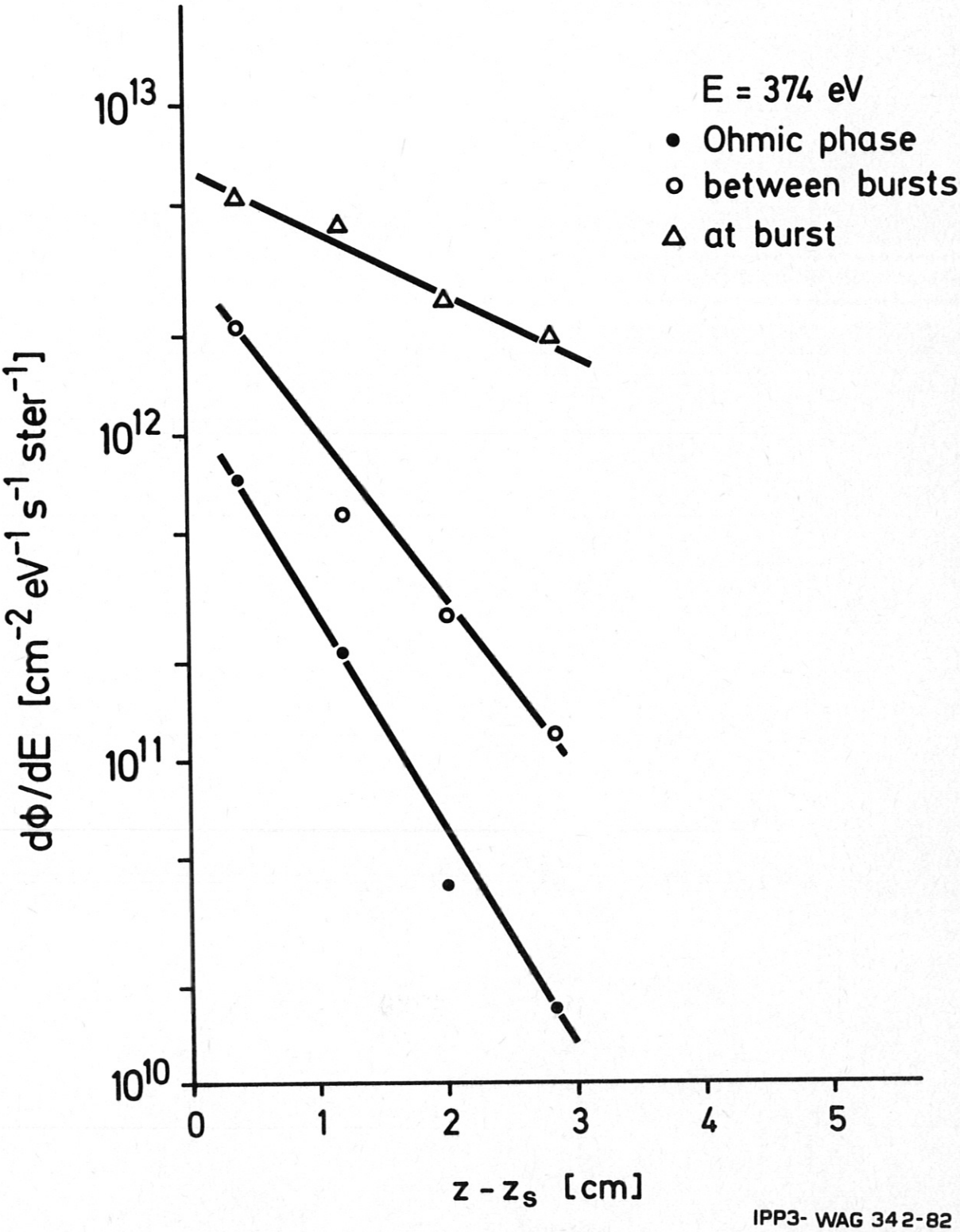
E = 374 eV
• Ohmic phase
o between bursts
Δ at burst
10^{13}
10^{12}
10^{11}
10^{10}
$d\Phi/dE$ [$cm^{-2} eV^{-1} s^{-1} ster^{-1}$]
0
1
2
3
4
5
$z - z_s$ [cm]
IPP3- WAG 342-82

Fig. 19